Antimicrobial Activity and Hemocompatibility of Zinc-Doped-Iron Oxide Nanoparticles

By

Nazifa Tabassum Tasnim
19126052

Nushrat Ferdous
20126014

A thesis submitted to the Department of Mathematics and Natural Sciences in partial fulfillment of the requirements for the degree of
Bachelor of Science in Microbiology

Department of Mathematics and Natural Sciences
Brac University
July 2023

Declaration

It is hereby declared that

1. The thesis submitted is my/our own original work while completing degree at Brac University.
2. The thesis does not contain material previously published or written by a third party, except where this is appropriately cited through full and accurate referencing.
3. The thesis does not contain material which has been accepted, or submitted, for any other degree or diploma at a university or other institution.
4. I/We have acknowledged all main sources of help.

Student's Full Name & Signature:

Nazifa Tabassum Tasnim	**Nushrat Ferdous**
19126052	20126014

Approval

The thesis/project titled "Antimicrobial Activity and Hemocompatibility of Zinc-Doped-Iron Oxide Nanoparticles" submitted by

1. Nazifa Tabassum Tasnim (19126052)
2. Nushrat Ferdous (20126014)

Of Summer, 2023 has been accepted as satisfactory in partial fulfillment of the requirement for the degree of Bachelor of Science in Microbiology on 20th July, 2023.

Examining Committee:

Supervisor:
(Member)

_____
Md. Salman Shakil
Senior Lecturer
Department of Mathematics and Natural Sciences
Brac University

Program Coordinator:
(Member)

_____
Nadia Sultana Deen, PhD
Associate Professor
Department of Mathematics and Natural Sciences
Brac University

Departmental Head:
(Chair)

_____
A F M Yusuf Haider, PhD
Professor and Chairperson
Department of Mathematics and Natural Sciences
Brac University

Ethics Statement

Our thesis paper contains less than 20% plagiarism.

Abstract/Executive Summary

Antibiotic resistance has been estimated to cause 10 million deaths worldwide by the year 2050. Given the severity of drug resistance, researchers are developing more efficient antibacterial methods. Over the last few years, iron oxide nanoparticles (IONPs) have drawn attention in treatment of microbial infections. However, the antimicrobial activity of IONPs can be enhanced by doping metals like zinc due to its own antimicrobial activity. In this study, we reported the antimicrobial activity and hemocompatibility of zinc-doped iron oxide nanoparticles (ZDI) synthesized via co-precipitation method. FTIR analysis confirmed that ZDI showed all the characteristics peak. Furthermore, ZDI exhibited antimicrobial activity against both gram-positive and gram-negative bacteria, with a maximal zone of inhibition (ZOI) of 18 mm against *Bacillus subtilis at* 15 mg/mL. Furthermore, MIC and IC_{50} results confirmed that ZDI were more potent in inhibiting the growth of gram-positive bacteria. Moreover, ZDI exhibited excellent hemocompatibility towards human red blood cells (≤ 5% hemolysis) at lower concentrations (upto 10 mg/mL).

Keywords: Zn-doped-iron oxide nanoparticles; Co-precipitation; Antimicrobial activity; Resistant bacteria; Nanoparticles; Hemolysis.

Acknowledgement

First and foremost, all praises to the Almighty for His consent through the journey. Then, we would like to express our deepest appreciation and respect to our advisor, Md. Salman Shakil, for his unwavering support, insightful advice, inspiration, and enthusiasm as well as for sharing his immense knowledge to help us complete our B.Sc. (Microbiology) thesis. We especially appreciate the thoughtful comments made at lab meetings. Our ability to manage challenging circumstances has always been improved by your professionalism and helpful feedback. We also are grateful for your enormous patience with us throughout the journey. We are truly grateful to him.

We would also like to thank our respected faculties specially Md. Mahamudul Hasan Rumon, Fahmida Sultana, Akash Ahmed, Dr. Zayed Bin Zakir and Dr. Mahboob Hossain, for guiding us and sharing valuable thoughts. Our special thanks to the Department of Mathematics and Natural Sciences for providing samples and instruments. Our heartiest thanks to Banik for donating blood for hemolysis assay. We are also grateful to Lab Officers, Shamima Akher and Md Mahmudul Hasan for helping us through the ups and downs. Especially, we would like to thank our seniors, Amrin and Arav for teaching us the core methods, knowledge sharing, continuous motivation, and inspiration.

We appreciate our friendly lab colleagues (Rodela, Dola, Ramisa, Nafisa, Safwan, Anchol, Tonuka, Zwad, Shuborna) and postgrads (Aziz, Shomnath, Nishat) for their insightful comments, motivation, and guidance. We are also thankful to our friends Jawad, Ahbab, Mowree, Fariha Shaira, Eusra, Agomoni, Srijila, Valentina and Ifrit for their constant support. We extend our gratitude to Kishan, Shadman and Abed for the reality check which really boosted our confidence and made us strong-willed. We also appreciate the continuous support from the administrative staff, and especially Ashik and Tanjila. Lastly, we recall all of our former mentors, seniors, juniors, and peers who never failed to motivate and encourage us. Above all, we owe our family, especially our parents, a huge debt of gratitude for their unwavering love and support over the years.

Table of Contents

List of Tables

List of Figures

List of Acronyms

AMR Antimicrobial Resistance

IONPs Iron Oxide Nanoparticles

ZDI Zinc Doped Iron Oxide Nanoparticles

ROS Reactive Oxygen Species

AMX Amoxicillin

MT Metronidazol

PEG Polyethylene Glycol

FTIR Fourier Transform Infrared

TEM Transmission Electron Microscopy

MRI Magnetic Resonance Imaging

ZOI Zone of Inhibition

MIC Minimum Inhibitory Concentration

MBC Minimum Bactericidal Concentration

MO Metal Oxides

RBC Red Blood Cell

PBS Phosphate-buffered Saline

NPs Nanoparticles

ROS Reactive oxygen species

Ref. References

Conc. Concentrations

NR Not reported

NDI Ni-doped-Fe_2O_4

NDIZ Ni-doped-Fe_3O_4/ZnO

CDI Cu-doped-α-Fe_2O_3

CBDI Co-doped-Fe_3O_4

ZDI Zn-doped-Fe_2O_3

ZODI ZnO-doped-Fe_3O_4

SDI Se-doped-Fe_3O_4

RDI Cr-doped-$CeFe_2O_4$

KDI Ca-doped-Fe_3O_4

MDI Mo-doped-Fe_3O_4

ADI Au-doped-Fe_3O_4

PEI Polyethylenimine

MAP Microwave-assisted process

CP Co-precipitation

GC Green combustion

CPA Chemical polymerization approach

SGP Sol-gel process

HDA Hydrothermal approach

STM Solvothermal method

NDG Nitrogen-doped grapheme

CLP Calcium phosphates

DLM D, l-methionine.

Chapter 1

1 Introduction

1.1 Epidemiology of Antimicrobial Resistance

Antimicrobial resistance (AMR) is an urgent public health threat associated with severe mortality and morbidity (Tacconelli & Pezzani, 2019). Nearly, 700,000 death occurrences are recorded due to AMR of various types of bacteria and this statistic is estimated to cross 10 million prior to the year 2050 (O'Neill, 2016). The estimated death occurrence is 4,730,000 in Asia, 390,000 in Europe, 4,150,000 in Africa, 317, 000 in North America , 392,000 in Latin America, and lastly, 22,000 in Oceania by 2050 (Neely & Holder, 1999). According to European Centre for Disease Prevention and Control, 33000 deaths have occurred due to antibiotic resistance before covid-19and 35,900 deaths occur every year solely in the United States ("Antibiotic resistance threats in the United States, 2019," 2019). The rate and incidence of antibiotic resistance in different countries varied greatly (Figure 1 and Table 1).

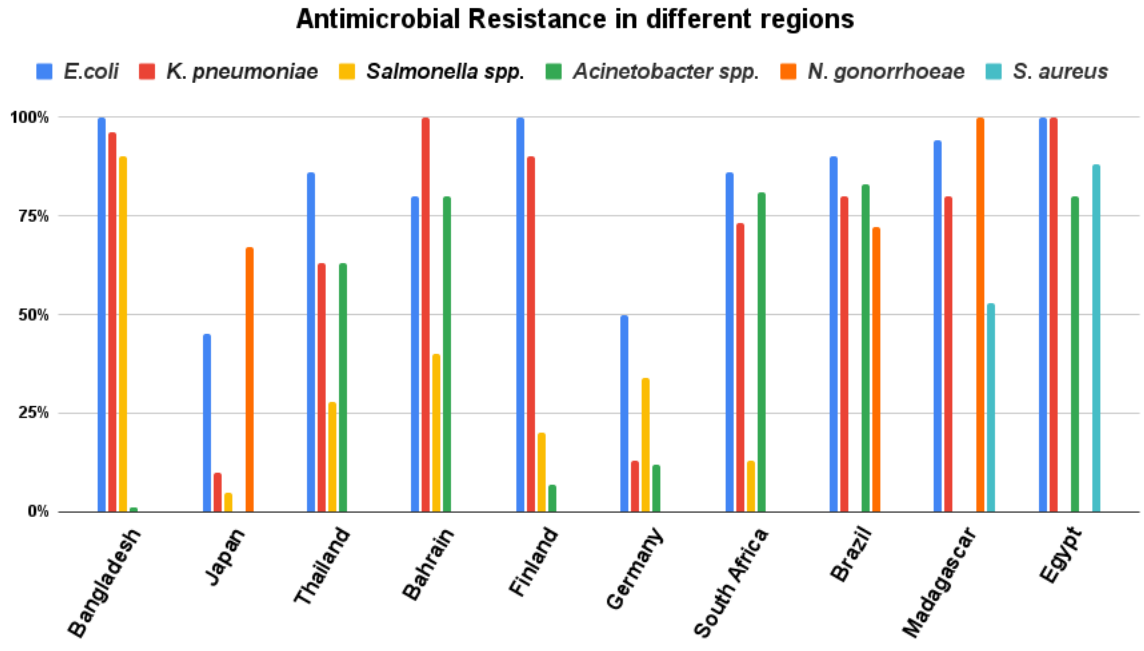

Figure 1: AMR in different regions. AMR: Antimicrobial resistance.

Table 1:Antimicrobial resistance in different regions(Organization, 2021).

Country	Bacteria	Infected number	Rate	Antibiotics
Bangladesh	*E. coli*	412	7-100%	CFPM, CFZ, AMP, CIP, MEM, IPM, CRO, LVX.
	K. pneumoniae	106	6-96%	CFZ, CTX, CIP, IPM.
	Salmonella spp.	20	0-90%	CTX, CFZ, CRO, CIP, ETP, MEM.
	Acinetobacter spp.	375,822	0–1%	AK, IPM, MEM, MIN.
Japan	*E. coli*	105,099	0–45%	AMP, CPFM, CTX, CFZ, CRO, CIP, IPM, LVX, MEM.
	K. pneumoniae	306	0–10%	CPFM, CTX, CFZ, CRO, IPM, LVX, MEM, CIP.
	Neisseria gonorrhoeae	1621	0–67%	AZM, CFZ, CRO, CIP, SPT.
	Salmonella spp.	103,744	0–5%	CFZ, CTX, CIP, IPM, MEM.
Thailand	*E. coli*	1007	0–86%	CPFM, CTX, CFZ, CRO, CIP, SXT, AMP, IPM, MEM, ERT, LVX, CL, DOR.
	Acinetobacter spp.	6907	1–63%	IPM, MEM, GM, AK, CL, DOR, TIG.
	K. pneumoniae	3225	0–63%	CPFM, CTX, CFZ, CRO, CIP, IPM, MEM, ERT, DOR, STX, CL, LVX.
	Salmonella spp.	2633	0–28%	CTX, CFZ, CRO, CIP, IPM, MEM, ERT, DOR.
Bahrain	*E. coli*	1101	0–80%	CPFM, CTX, CFZ, CRO, CIP, IPM, MEM, ERT, DOR, STX, CL, LVX.
	Acinetobacter spp.	204	0–80%	AK, CL, GM, IPM, MEM, TIG.
	K. pneumoniae	289	0–100%	CPFM, CTX, CFZ, CRO, CIP, IPM, MEM, ERT, STX, CL, LVX.
	Salmonella spp.	250	0–40%	CFZ, CRO, CIP, IPM, MEM.
Finland	*E. coli*	1544	0–100%	CTX, CFZ, CRO, CIP, IPM, MEM, ERT, STX, LVX, AMP.
	Acinetobacter spp.	15,983	0–7%	MEM.
	K. pneumoniae	6853	0–90%	CTX, CFZ, CRO, CIP, IPM, MEM, ERT, STX, LVX.
	Salmonella spp.	159,676	0–20%	CRO, CIP, MEM, CFZ, LVX.
Germany	*E. coli*	61,112	0–50%	CTX, CFZ, CRO, CIP, AMP, IPM, MEM, ERT, STX, LVX.
	Acinetobacter spp.	357,718	0–12%	IPM, MEM, GM, AK.
	K. pneumoniae	23,837	0–13%	CPFM, CTX, CFZ, CRO, CIP, IPM, MEM, ERT, LVX.
	Salmonella spp.	11,015	0–34%	CTX, CFZ, CRO, CIP, IPM, MEM, ERT, LVX.
South Africa	*E. coli*	6965	0–86%	CPFM, CTX, CFZ, CRO, CIP, IPM, MEM, ERT, DOR, STX, AMP.
	Acinetobacter spp.	5983	0–81%	AK, GM, IPM, MEM, MIN, TIG.
	K. pneumoniae	1228	13–73%	CPFM, CFZ, CRO, CIP, IPM, MEM, ERT, STX.
	Salmonella spp.	3138	0–13%	CTX, CFZ, CRO, CIP, IPM, ERT.
Brazil	*E. coli*	862	0–90%	CTX, CFZ, CRO, CIP, IPM, MEM, ERT, LVX, AMP, STX.
	Acinetobacter spp.	860	0–83%	AK, GM, IPM, MEM, TIG.
	K. pneumoniae	376	19–80%	CTX, CFZ, CRO, CIP, IPM, MEM, ERT, LVX, STX.
	N. gonorrhoeae	6	0–72%	CPME, CRO, CIP, GM, SPT.
Madagascar	*E. coli*	2011	0–94%	CPFM, CTX, CFZ, CRO, CIP, IPM, MEM, ERT, DOR, STX, AMP, LVX.

	K. pneumoniae	39	0–80%	CPFM, CTX, CFZ, CRO, STX, CL, IPM.
	S. aureus	5	18–53%	FOX.
	N. gonorrhoeae	446	1–100%	CRO, CIP, AZM.
Egypt	*Acinetobacter* spp.	46	6–80%	AK, CL, GM, IPM, MEM.
	E. coli	622	4–100%	CPFM, CTX, CFZ, CRO, IPM, MEM, ERT, AMP, LVX, CIP.
	K. pneumoniae	149	38–100%	CPFM, CTX, CFZ, CRO, CIP, IPM, MEM, ERT, DOR, STX, LVX.
	S. aureus	46	66–88%	OXA.

CFPM: Cefepime; CFZ: Cetadizime; AMP: Ampicillin; CIP: Ciprofloxacin; MEM: Meropenem; IPM: Imipenem; CRO: Ceftriaxone; LVX: Levofloxacin; CTX: Cefotaxime; ETP: Ertapenem; SPT: Spectinomycin; Co-trimoxazole: SXT; GM: Gentamicin; DOR: Doripenem; TIG: Tigecycline; CL: Colistin; AK: Amikacin; MIN: Minocycline; AZM: Azithromycin; FOX: Cefoxitin; OXA: Oxacillin.

Apart from the uncontrolled use of antibiotics, other factors including not maintaining good hygiene, poor healthcare system, usage of antibiotics in the livestock and food industries and accumulation in the environment contribute to AMR as well (Collignon & Beggs, 2019). Unfortunately, in the past few decades, bacteria have developed a wide array of AMR mechanisms protecting them from the effects of these drugs and as a result, AMR became more prevalent (Aslam *et al*., 2018). Mainly resistance mechanisms are divided into three different pathways; altering the antibiotic target site, modifying the antibiotic molecule as well as destroying it, and inhibiting the antibiotic molecule from binding to target sites (Blair *et al*., 2015; Wright, 2010). Given the severity of drug resistance and the scarcity of therapeutic choices, researchers are developing more efficient and enduring antibacterial methods. Recently, nanoparticles have drawn attention in the treatment of microbial infections (Arakha *et al*., 2015; Farias *et al*., 2018; Hussein-Al-Ali *et al*., 2014; Jain *et al*., 2021; Lallo da Silva *et al*., 2019; Mussin *et al*., 2021; Vazquez-Muñoz *et al*., 2019; Yu *et al*., 2020) and there is a variety of ways to overcome the mechanisms of microbial resistance, including hindering the formation of biofilms, disrupting membranes by generating reactive oxygen species (ROS), and concurrently acting on numerous modes of action to stop microbial growth. It occurs since most nanoparticles do not function through the same channels that most antibiotic resistance mechanisms do (Rai, 2013).

1.2 Nanoparticles and Pathogenic Bacteria: An Alternative Antimicrobial Agent

The effect of nanoparticles to bacteria varies by strain or species (Baek & An, 2011; Hajipour et al., 2012). One of the major reasons why pathogens are prone to nanoparticles could be their cell wall and cell membrane composition (de Lacerda Coriolano *et al.*, 2021; Pokhrel et al., 2022). Azam *et al.* (2012) and Ismail *et al.* (2015) have found that gram-positive bacteria are more susceptible to IONPs than gram-negative bacteria, and this difference has been related to the polarity of cell wall and cell membrane (Azam et al., 2012; Ismail *et al.*, 2015). Gram-negative bacteria's cell wall is more physically and chemically complicated than gram-positive bacteria's, with an outer membrane that is composed of lipopolysaccharides, phospholipids, and proteins and an underneath thin peptidoglycan layer (Aruguete & Hochella, 2010). The outer membrane of gram-negative bacteria is reported to contain lipopolysaccharides, which elevate the net negative charge of the cell membrane (Hajipour *et al.*, 2012), this would render the cell membrane that is impermeable to lipophilic solutes while also limiting negatively charged free radical penetration. As a result, gram-negative bacteria are claimed to be lesser susceptible to IONPs (Ismail *et al.*, 2015). Contrary to gram-positive bacteria that lack an outer membrane and rely only on the peptidoglycan layer, which is not a robust permeable barrier, are more vulnerable to lower nanoparticles concentrations (Bhattacharya & Neogi, 2018). Recently, among all the nanoparticles, iron oxide nanoparticles (IONPs) are particularly interesting in developing therapies, targeted drug delivery, and other biological applications due to their antimicrobial activity, attractive magnetic properties, vast surface area, tiny size, minimal cytotoxicity, and biocompatibility (Arakha *et al.*, 2015; Das *et al.*, 2020; Hussein-Al-Ali *et al.*, 2014; Yu *et al.*, 2020).

1.3 Iron Oxide Nanoparticles (IONPs)

IONPs belonging to the ferrimagnetic class of magnetic materials are used for a wide variety of biomedical and bio-engineering applications (Albert *et al.*, 2010). IONPs synthesis methods include co-precipitation (CP) (Bhushan *et al.*, 2019), thermal decomposition (Rabia *et al.*, 2017), the sol–gel process (SGP) (Toropova *et al.*, 2021), hydrothermal approach (HTM)(Li et al., 2020), electrochemical method (Prabhu et al., 2015), laser ablation (Omelchenko *et al.*, 2015;

Rabia *et al.*, 2017) sonochemical, microwave, micro emulsion methods, the matrix-mediated method using PVA, "green synthesis", and many more (Arias *et al.*, 2018; Armijo *et al.*, 2020; Rufus *et al.*, 2016; Tran *et al.*, 2010). Different polymorphic forms of iron oxides include γ-Fe_2O_3, Fe_3O_4, and FeO which are respectively maghemite, magnetite, and wustite. The most studied are γ-Fe_2O_3 and Fe_3O_4 because they possess extraordinary properties at the nanoscale e.g. superparamagnetism, high specific surface area, biocompatible, etc. (Noqta *et al.*, 2019). At this scale, quantum phenomena have an impact on the optical, electrical, and magnetic properties of matter (Iriarte-Mesa *et al.*, 2020; Trindade & Thomas, 2013; Tringides *et al.*, 2007). For instance, the magnetic Fe_3O_4 nanoparticles below the size of 20 nm are superparamagnetic (Li *et al.*, 2017). The increased surface area-to-volume ratio enables excellent dispersibility in a solution form which makes these materials ideal for surface functionalization and modification in a variety of applications, including separation techniques (Gu *et al.*, 2006), visualization and diagnostics (Jacinto *et al.*, 2021), magnetic sorting (of cells and other biomolecules, etc.) (Lin *et al.*, 2017), drug delivery (Saikia *et al.*, 2016), cancer hyperthermia (Zhang & Song, 2016), sensing, etc. (Ajinkya *et al*., 2020; Gawande *et al*., 2016). Additionally, IONPs and free iron ions exhibit antimicrobial properties; however, unlike free ions, IONPs do not possess a significant toxic effect on mammalian cells (D. Li *et al.*, 2021; Du Li *et al.*, 2021; Saliani *et al.*, 2015a, 2015b; Sihem *et al.*, 2020). Bare IONPs, however, fall short of what is needed for practical applications. One of the most popular and straightforward methods for obtaining enhanced multifunctional characteristics in IONPs is doping (Laha *et al.*, 2022; Liu *et al.*, 2016).

1.4 Doped Iron Oxide Nanoparticles (Doped-IONPs)

Doped-IONPs are synthesized following the modern doping procedure approach to alter the physicochemical as well as biological, electrical and optical properties. Doping is inserting foreign metal particles into an empty crystal lattice of another metal which changes the primary metal's various properties (Rekha *et al.*, 2010). Multiple types of dopants e.g. manganese (Mn), zinc (Zn), silver (Ag), cobalt (Co), nickel (Ni), gold (Au), copper (Cu), rare earth and different synthesis methods are broadly applied for doping purposes (Zhang et al., 2006). However, selecting a proper dopant is crucial as excessive amounts of doping can deteriorate the catalyst performance caused by the high accumulation of dopant on the catalyst itself (Mohtar *et al*., 2021). Different doping methods include CP, green-synthesis, combustion, SGP, sonochemical,

laser ablation and biological reduction (Karunakaran *et al*., 2010; Khan et al., 2020; Khashan et al., 2020). The green-synthesis method for doping is eco-friendly producing fewer pollutants (Hamidian *et al*., 2022).

Recently, doping has had more significance in biomedical applications including drug delivery, antimicrobial and anti-cancer activities observation (Cui et al., 2021; Shoaib *et al*., 2021). A recent study reported the addition of transition metals into IONPs exhibited better antimicrobial activity than bare IONPs (Elayakumar *et al.*, 2019). Such advantages emerge due to metals (e.g. Zn, Ag, and Cu) having antimicrobial characteristics in their bulk form (J. T. Seil & T. J. Webster, 2012). Additionally, the antimicrobial activity of these metals is inversely related to their nanoscale diameters (Justin T. Seil & Thomas J. Webster, 2012). Doping aids in increasing the surface area, improving the loading capability according to the desired size, shape and properties results in potential tumor killing agents (Cui *et al*., 2021). The chemotherapeutic actions can be modified and controlled as well (Liu et al., 2021). Study by Casula *et al.* (2016) showed the bare IONPs can obtain intrinsic magnetic properties along with desired morphological and structural features by Mn doping (Casula *et al.*, 2016). Studies reported that metal doped-IONPs minimized the proliferation of both gram-positive and gram-negative bacterial strains such as *S. aureus* (Bhushan et al., 2019), *E. coli* (Anbu, 2022; Bhushan *et al*., 2019) and *Serratia marcescens* (Raveesha et al., 2021). In another research by Ahghari *et al.*(2013), doped-IONPs showed enhanced antimicrobial activity than bare IONPs (Ahghari *et al*., 2023).

1.4.1 Antimicrobial Activities of Doped-IONPs

Bare IONPs have their own properties which can be enhanced by doping (Keerthana *et al*., 2021). Although IONPs have its own anti-bacterial activities, doping through different methods can change several properties e.g. increasing their antibacterial activities and displaying cytotoxic activity (Keerthana *et al.*, 2021). IONPs doped with transition metals and coating material shows significant antimicrobial activity based on synthesis process, size, and concentrations on gram-positive and gram-negative bacteria (Table 2). Different studies of doped-IONPs sized between 5-500 nm exhibited improved antimicrobial activity against both gram-positive and gram-negative bacteria. Doped-IONPs sized around 20-200 nm have shown notable antimicrobial activity on different bacteria, where doped-IONPs size less than 20 nm

(Janczak *et al*., 2021; Rahdar *et al.*, 2020; Sadeghi Rad *et al*., 2021) and larger than 200 nm are comparatively insignificant (Anbu, 2022; Babu *et al*., 2020; Haghniaz *et al*., 2021; Janczak *et al*., 2021; Raveesha *et al.*, 2021; Vijayalakshmi & L, 2021). Doped-IONPs were synthesized by using CP, chemical polymerization approach (CPA), microwave-assisted approach (MAP), green combustion (GC), SGP, HTM and solvothermal method (STM) although CP method was the most approached one due to its less complexity (Anbu, 2022; Babu *et al.*, 2020; Bhushan *et al.*, 2019; Haghniaz *et al.*, 2021; Vijayalakshmi & L, 2021). The core advantage of the CP methods than other synthesis method is the ability to produce a large amount of nanoparticles. The size and shape of the nanoparticles can be customized with reasonable success using the CP approach by altering ionic strength, pH, temperature, the type of the salts e.g. chlorides, perchlorates, nitrates, and sulfates, or the concentration ratio of FeII/FeIII (Babes *et al.*, 1999). According to the thermodynamics of the CP process, full IONP precipitation should be expected in a non-oxidizing oxygen environment with a pH range of 8 to 14, and in a stoichiometric ratio of 2:1 (Fe^{3+}/Fe^{2+}) (Jolivet *et al.*, 2004). Additionally, the size of the particles can be controlled by changing or adding different stabilizers and Fe_3O_4 ratios (Liu *et al.*, 2004). In this study, CP synthesis method has been used to its adverse flexibilities.

Metal doped with IONPs e.g. Zn-doped-IONPs (ZDI), Cu-doped-IONPs (CDI), Ni-doped-IONPs (NDI), Se-doped-IONPs (SDI), Au-doped-IONPs, Cr-doped-IONPs, and Ca-doped-IONPs (KDI) have shown higher antimicrobial activity against resistant bacteria (*Bacillus subtilis, K. pneumoniae, E. coli, S. aureus, Proteus vulgaris*) compared to Mo-doped-IONPs (MDI), Co-doped-IONPs (CBDI), in terms of zone of inhibition (ZOI) (Table 2). Among all the metal-doped-IONPs ZDI, CDI, SDI have shown the highest bacterial inhibition based on ZOI (≥ 20 nm) (Ahghari *et al*., 2023; Babu *et al*., 2020; Raveesha *et al.*, 2021), while KDI, MDI, CBDI have shown the lowest ZOI against different bacteria (except on *S. aureus)* (Adamiano *et al*., 2019; Rahdar et al., 2020; Shujah *et al*., 2022; Vijayalakshmi & L, 2021). Doping activity of ZDI at the lowest concentration was comparatively higher than any other doped-IONPs *(Haghniaz et al*., 2021). Apart from ZOI, minimum inhibitory concentration (MIC) was performed to determine the lowest concentration which could inhibit the bacterial growth (Anbu, 2022; Haghniaz *et al*., 2021; Rahdar *et al.*, 2020; Raveesha *et al.*, 2021; Shujah *et al.*, 2022; Vijayalakshmi & L, 2021).

Table 2: List of particles size, synthesis methods, coating materials, MIC, MBC, ZOI and mechanisms of doped-IONPs on different organisms.

DMP	NPs	Size (nm)	SYM	CMM	Organisms	Conc. of NPs (µg/mL)	ZOI (mm)	MIC (µg/mL)	MBC (µg/mL)	Mechanisms	Ref.
Ni	NDI	15-200	CPA	NDG	*E. coli*	50	16	50	NR	Ni^{2+} and Fe^{3+} ions interact with membrane proteins, inflicting damage to the bacterial membrane and inhibiting bacterial growth.	(Anbu, 2022)
				Cellulose	*B. subtilis*	50	14	50	NR		
	NDIZ	28-33	MAP	ZnO	*K. pneumoniae*	NR	13	NR	NR	The microwave and sonication of Fe_3O_4/ZnO nanocomposites and different NDIZ had a significant impact on ROS assisted toxicity. The ultrasonication process allows Ni ions to reach the Fe_3O_4/ZnO surface and generate greater ROS in the solution. This triggered oxidative stress in the bacteria, which results in cell disintegration.	(Vijayalakshmi & L, 2021)
					S. aureus	NR	17	NR	NR		
	NDIZ	36	MAP	ZnO	*K. pneumoniae*	NR	6	NR	NR		
					S. aureus	NR	6	NR	NR		
Cu	CDI	20–60	GC	PEI	*P. vulgaris*	400	16 ± 1.0	250	NR	Particles disrupt the cell wall, inducing oxidative stress and cell lysis. It promotes the oxidation of proteins and DNA by producing ROS.	(Raveesha *et al.*, 2021)
					Serratia marcescens	400	16.67 ± 0.58	250	NR		
					Streptococcus mutants	400	10	250	NR		
					Bacillus cereus	400	15 ± 1.0	NR	NR		

	CDI	21	CP	NR	*E. coli*	400	20	600	NR	ROS formation which causes oxidative stress. Free radicals lead to bacterial death by acting in several ways which include breaking of DNA strands, peroxidation of membrane lipids, inactivation of enzymes and depolymerization of polysaccharides,	(Bhushan *et al*., 2019)
						600	23± 1				
						800	25				
					B. subtilis	400	16	600	NR		
						600	19				
						800	23				
					S. aureus	400	18	750	NR		
						600	18				
						800	20				
					Salmonella typhi	400	15 ± 1.0	600	NR		
						600	20 ± 1.0				
						800	23				
Co	CBDI	10-14	CP	NR	*Shigella dysenteriae*	1-2048	NR	>2048	>2048	The particles attach to the plasma membrane causing disruption and ensuring the ROS are already co-localized to the lipids. But the electron emitted from the iron atom in the presence of cobalt (III) (Co) might be retained by the Co (III) and converted to the highly stable Co (II)and causing no formation of highly oxidized species and less activity.	(Rahdar *et al*., 2020)
					K. pneumoniae	1-2048	NR	>2048	>2048		
					Acenetobacter baumnii	1-2048	NR	>2048	>2048		
					Streptococcus pyogene	1-2048	NR	>2048	>2048		
Zn	ZDI	5–15	N/A	NR	*E. coli*	NR	NR	NR	NR	Induce oxidative stress and destabilize the cellular redox system, resulting in the production of reactive	(Janczak *et al*., 2021)
					S. aureus	NR	NR	NR	NR		
					Pseudomonas aeruginosa	NR	NR	NR	NR		
					Legionella pneumophila	NR	NR	NR	NR		
					Salmonella enterica	NR	NR	NR	NR		

										oxygen species.	
	ZODI	75.90	CP	NR	*E. coli*	250000	14	NR	NR	Positively charged metal nanoparticles and negatively charged microorganisms are attracted to one another. Consequently, the bacteria are oxidized and exterminated. Cell cleavage causes an interaction between metal ions and thiol groups on the bacterial cell surface. Another route for bacterial protein and DNA damage might be ROS including OH, O_2, and H_2O_2.	(Babu *et al*., 2020)
					S. aureus	250000	10	NR	NR		
	ZODI	34.99	CP	Ag	*E. coli*	250000	19	NR	NR	ZnO-based nanocomposites aggregate in the outer membrane or cytoplasm of bacterial cells. This leads to the discharge of Zn^{2+} ions, which promotes cell membrane damage and the death of bacterial cells.	(Babu *et al*., 2020)
					S. aureus	250000	11	NR	NR		
	ZDI	500	STM	NR	*Microcystis aeruginosa*	50000	NR	NR	NR	Magnetic Zn-doped Fe_3O_4 particles have a photocatalytic inactivation effect. The photocatalytic	(Qi *et al.*, 2020)

										pretreatment produced superoxide radicals, which were responsible for mucilage desorption. As a result, the improved cell removal may be explained through the mucilage desorption impact on microorganisms in the photocatalytic process.	
	ZDI	28	SGP	NR	*K. pneumoniae*	25	16	75	NR	Generate ROS-induced bacterial harm. Following that, intracellular cytoplasmic leakage of sugar and protein indicates their potential to disrupt bacterial membrane integrity.	(Sharma *et al*., 2022)
						50					
						75					
	ZDI	47.9 ±2.5	CP	NR	*E. coli*	12.5	9 ± 0.8	NR	NR	Induced bacterial cell death via membrane disruption, protein leakage, and ROS generation for bactericidal efficacy. Small NPs adsorbing on the cell surface can generate intracellular ROS, leading to bacterial cell death.	(Haghniaz *et al*., 2021)
						25	10 ± 0.4				
						50	10 ± 0.6				
						100	11 ± 0.7				
					P. aeruginosa	12.5	10 ± 0.8				
						25	11 ± 0.4				
						50	11 ± 0.5				
						100	12 ± 0.8				
					K. pneumoniae	12.5	10 ± 0.5				
						25	10 ± 1				
						50	11 ± 1.1				
						100	13 ± 1.6				
					S. typhi	12.5	8 ± 0.5				
						25	10 ± 0.7				

						50	11 ± 1.4				
						100	12 ± 1.1				
					S. aureus	12.5	10 ± 0.5				
						25	10 ± 0.6				
						50	11 ± 0.8				
						100	13 ± 0.9				
Se	SDI	80	CP	NR	*S. aureus*	10000	18	NR	NR	The combination of Se NPs effectively increases the formation of ROS. The most commonly acknowledged mode of action for Se NPs is particle attachment to the bacterial surface and selenium ion release into the bacterial cell, resulting in oxidative stress, protein synthesis inhibition, or DNA mutation.	(Ahghari *et al*., 2023)
					Staphylococcus saprophyticus	10000	2	NR	NR		
					P. aeruginosa	10000	8	NR	NR		
					K. pneumoniae	10000	6	NR	NR		
					E. coli	10000	11	NR	NR		
Cr	RDI	1.64	CP	NR	*S. aureus* (ATCC 25993)	800	NR	10	200	The major mechanism could be oxidative stress triggered by ROS such as superoxide radicals, hydroxyl radicals, and hydrogen peroxide (H_2O_2), which can damage bacteria's DNA and proteins. In this case, magnetite may be regarded as the source of the ROS that reduced the	(Sadeghi Rad *et al*., 2021)
								50	400		

										viability of *S. aureus*. Additionally, the use of transition metals, particularly chromium, can affect the topology and adversely affect bacteria's replication and transcription.	
Ca	KDI	5–10	CP	CLP	*E. coli*	5000	NR	NR	NR	Dose dependent toxicity of NPs leads to bacterial cell rupture.	(Adamiano *et al*., 2019)
					S. aureus	5000	NR	NR			
					Salmonella enteritidis	5000	NR	NR			
					P. aeruginosa	5000	NR	NR			
Mo	MDI	36.11	CP	NR	*E. coli*	20000	3.45	NR	NR	By ROS formation, positive radicals rapidly enter into bacterial cell membranes, causing bacterial death. In contrast to negatively charged radicals such as hydroxyl radicals and superoxide anions, which are unable to to pass through microorganism cell membranes yet cause significant damage to the outermost surface of bacterial cells.	(Shujah *et al*., 2022)
		38.45									
		25.74									
		24.38				400000	1.45	NR	NR		
Au	ADI	11.9 ± 0.15	HDA	DLM	*A.baumannii*	70000	NR	NR	NR	Strong ionic contact of nanoparticles with bacterial cell membrane increases the permeability which leads to cell death.	(Žalnėravičius *et al*., 2019)
					S.enterica	70000	NR	NR	NR		
					S.aureus	70000	NR	NR	NR		
					Micrococcus luteus	70000	NR	NR	NR		

DMP: Doping materials; SYM: Synthesis Methods; CMM: Coating materials; NPs: Nanoparticles; Ref.: References; Conc.: Concentrations; ZOI: Zone of inhibition; MIC: Minimum inhibitory concentration; MBC: Minimum bactericidal concentration; NR: Not reported; ROS: Reactive oxygen species; NDI: Ni-doped-Fe_2O_4;NDIZ: Ni-doped-Fe_3O_4/ZnO; CDI: Cu-doped-α-Fe_2O_3; CBDI: Co-doped-Fe_3O_4; ZDI: Zn-doped-Fe_2O_3; ZODI: ZnO-doped-Fe_3O_4; SDI: Se-doped-Fe_3O_4; RDI: Cr-doped-$CeFe_2O_4$; KDI: Ca-doped-Fe_3O_4; MDI: Mo-doped-Fe_3O_4; ADI: Au-doped-Fe_3O_4;PEI: Polyethylenimine; OH: Hydroxyl radicals; O_2: Superoxide anion radicals; H_2O_2 : Hydrogen peroxide; MAP: Microwave-assisted process; CP: Co-precipitation; GC: Green combustion; CPA: Chemical polymerization approach; SGP: Sol-gel process; HDA: Hydrothermal approach; STM: Solvothermal method; NDG: Nitrogen-doped grapheme; CLP: Calcium phosphates; DLM: D,l-methionine.

Studies of NDI and ZDI had demonstrated better MIC with the lowest amount on *E. coli, B. subtilis, S. typhi, K. pneumonia* while MDI had shown no significant inhibition of *E. coli* at the highest concentration (Table 2) (Shujah et al., 2022). However, MIC and minimum bactericidal concentration (MBC) of doped-IONPs were not reported in most of the studies (Adamiano *et al*., 2019; Ahghari et al., 2023; Babu *et al.*, 2020; Haghniaz *et al.*, 2021; Janczak *et al.*, 2021; Qi *et al*., 2020; Shujah *et al.*, 2022; Vijayalakshmi & L, 2021; Žalnėravičius et al., 2019). Although research by Ivashchenko *et al*. (2015) represented a higher antimicrobial activity of doped-IONPs combined with antibiotics (Ivashchenko *et al.*, 2015). He also mentioned in a different study that doped-IONPs combined with antibiotics had released iron ions nearly twice as much as bare IONPs at pH 5 in response to the formation of galvanic couple with metal, leading to a better antimicrobial activity (Ivashchenko *et al.*, 2017). Doped-IONPs and bare IONPs had shared similar mechanism of actions from generating ROS to disrupt the bacterial cell membrane and DNA, eventually leading to the cell death (Adamiano *et al.*, 2019; Ahghari *et al.*, 2023; Babu *et al.*, 2020; Haghniaz *et al*., 2021; Janczak *et al.*, 2021; Qi *et al.*, 2020; Rahdar *et al.*, 2020; Sadeghi Rad *et al.*, 2021; Shujah *et al*., 2022; Vijayalakshmi & L, 2021; Žalnėravičius *et al*., 2019).

1.5 Zinc-Doped-Iron Oxide Nanoparticles (ZDI)

Zinc is required by microorganisms, and at relatively low endogenous amounts, they contribute to a variety of important reactions (Haase *et al.*, 2008; Leung *et al*., 2012). The disruption of Zn^{2+} homeostasis caused by an increase in Zn^{2+} concentration above optimum levels—typically between 10^{-7} M and 10^{-5} M depending on the microbial strains that allowed Zn^{2+} to enter cells and made zinc lethal to prokaryotes above a concentration of 10^{-4} M (Borovanský & Riley, 1989; Sugarman, 1983). As a result, Zn^{2+} exhibits antimicrobial activity and may have antibacterial properties. Two processes, both of which resulted in cell death, were used to account for their antibacterial actions. One resulted in a direct interaction with microbial membranes that

destabilized the membrane and increases permeability (Stanić *et al*., 2010). The other one was the interaction with nucleic acids and inactivation of respiratory system enzymes (Fang *et al.*, 2006).

Due to the lower toxicity of Zn^{2+}, ZDI had received a lot of interest in nanomedicine. Since the permitted reference daily intake values for Fe and Zn are 18 and 15 mg/day, respectively which is significantly greater than any other biocompatible substance—ZDI have been recognized as a promising choice for bio-medical applications (Hoque et al., 2013). Moreover, cell viability had been observed to be impacted by the physicochemical characteristics of nanoparticles, specifically size and specific surface area and it is well known that nanoscaled particles are much more threatening than micro-scaled ones (Y. Li et al., 2018; Zhang *et al.*, 2018). Doumandji *et al.* (2020) reported ZDI exhibited both the nanosheets and the spherical shape characteristic of IONPs and ZnO nanoparticles (Doumandji *et al.*, 2020). Another study by Abdel Maksoud *et al.* (2021) also reported that ZDI had shown incredible results as an antimicrobial agent(Abdel Maksoud *et al*., 2021). The mechanism of action(s) of ZDI are discussed below-

1.5.1 Mechanism of Actions of ZDI Antimicrobial Activity

Although doped-IONPs had been demonstrated to exhibit antimicrobial activity against a wide range of microorganisms, including gram-negative and gram-positive bacteria and fungi, little is understood about the exact mechanism of their mode of antimicrobial action. Nonetheless, substantial study had been conducted to understand their method of action, and four well-defined mechanisms had been postulated thus far: (i) oxidative stress by ROS generation, (ii) reduced expression of antibiotic resistance genes, protein and enzyme deactivation, (iii) disruption of cell wall and DNA replication and (iv) impairment of efflux pump (Figure 2).

1.5.1.1 Reactive Oxygen Species (ROS) Generation

ZDI exhibited similar mechanism of antimicrobial activity like bare IONPs where one of the important mechanism was generation of ROS (AlMatar *et al.*, 2018; Kohanski et al., 2010) including in photocatalysis, Fenton reactions, or similar ones (Silvia *et al.*, 2017). ROS having a genotoxic action, damage the DNA molecules (Kohanski *et al.*, 2010). The production of ROS leads to oxidative stress. Bacterial mortality is caused by free radicals in a variety of ways, including the depolymerization of polysaccharides, peroxidation of membrane lipids, breaking of

DNA strands, and inactivation of enzymes (Bhushan *et al.,* 2019). An activity reduction in the antioxidant systems enzymes such as catalase and glutathione reductase could be generated by an increase in ROS concentration (Janani *et al.*, 2021). Additionally, ZDI could destruct the integrity of bacterial cell membrane (Adamiano et al., 2019; Babu *et al.*, 2020).

The combination of foreign metals with nanoparticles by doping method could effectively increase the formation of ROS (Rayman, 2000). Besides that, with the addition of doped particles, the spherical morphology of nanoparticles can shift to a nano foil-like structure, which enhanced antimicrobial activity (Vijayalakshmi & L, 2021). In metal-based nanoparticles, it accumulated in the outer membrane or cytoplasm of bacterial cell which triggered the discharge of metal ions leading to cell membrane damage resulting in the death of bacterial cells (Dutta *et al.*, 2013; Jiang *et al.*, 2016; Shi *et al.*, 2014).

At the interface of ZDI , another mode of electron trapping could happen (Feng *et al.*, 2014). The reduction of Fe^{3+} ions to Fe^{2+} ions utilize the electrons from the Fermi energy level (the highest energy level an electron occupies at the absolute zero temperature) of metal oxide (e.g. ZnO) and thus decrease the rate of electron–hole recombination. The photocatalytic efficiency of the ternary nanocomposite enhanced by these electron trapping mechanisms (Babu *et al.,* 2020). Due to the lower stability of Fe^{2+} ions, they get oxidized immediately by oxygen molecules *(Ansari et al.*, 2013; Feng *et al.*, 2014; M. T. Bell *et al*., 1999). The electrons released during this oxidation reaction were used to form superoxide ion ($O_2{\cdot}^-$) and the holes generated at the IONPs form the Hydroxyl radical (OH·). The basic ROS (Babu *et al*., 2020) reaction process involves -

$$Fe^{3+} + e^- \rightarrow Fe^{2+} \quad \text{---------- (1)}$$

$$Fe^{2+} + O_2 \rightarrow Fe^{3+} + O_2{\bullet}^- \quad \text{---------- (2)}$$

$$A^{2+} + O_2{\bullet}^- \rightarrow A^{+} + O_2 \quad \text{---------- (3)}$$

$$Fe^{2+} + H_2O_2 \rightarrow Fe^{3+} + {\bullet}OH + OH^- \quad \text{---------- (4)}$$

$$O_2{\bullet}^- + H_2O_2 \rightarrow OH^- + {\bullet}OH \quad \text{---------- (5)}$$

Where ‘A’ represents all transition metals.

1.5.1.2 Reduced Expression of Antibiotic Resistance Genes, Protein and Enzyme Deactivation

Similar to bare IONPs , ZDI can also bind to mercapto (-SH), amino (-NH), and carboxyl (-COOH) functional groups of proteins, particularly those in enzymes, causing deactivation or partial inhibition and a decrease expression of antibiotic resistance genes in antibiotic-resistant bacteria (AlMatar *et al.*, 2018; Vedernikova, 2015; Yu *et al.*, 2015).

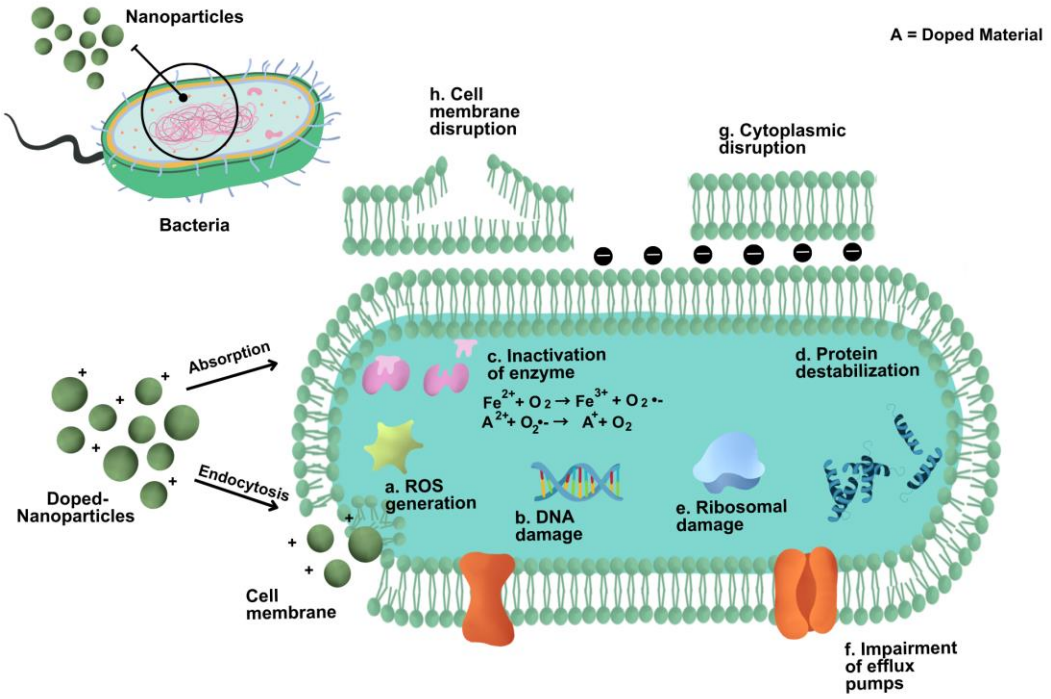

Figure 2: The mechanism of actions of doped-IONPs antimicrobial activity. Particles trigger oxidative stress and cell lysis by (a) generating ROS, (b) damaging DNA (c) inactivating enzymes, (d) destabilizing proteins, (e) damaging ribosome, (f) impairing efflux pump, (g) disrupting cytoplasm and (h) cell membrane. ROS: Reactive oxygen species; IONPs: Iron Oxide Nanoparticles.

1.5.1.3 Disruption of Cell Wall and DNA Replication

The use of transition metals by doping method, particularly chromium, can affect the topology and adversely affect bacteria's DNA replication and transcription (Plaper *et al.*, 2002; Vedernikova, 2015). Doped-IONPs can enter the cytoplasm (Božić *et al.*, 2020), accumulate there, and damage cell wall in the same way as bare IONPs *(Armijo et al., 2020; Yunqiao Li et al.*, 2018). Moreover, F0/F1-ATPase activity, the rate of H(+) channel through the membrane,

and the redox potential can all be affected (Gabrielyan *et al.*, 2019). Based on their size and similarities to other forms of metal IONPs, the antimicrobial effect of doped-IONPs has been the subject of various investigations (Babu *et al*., 2020).

1.5.1.4 Impairment of Efflux Pump

There are two potential ways that ZDI may prevent efflux pumps from functioning. One potential method is the direct binding of ZDI to the active site of efflux pumps, preventing the extrusion of antibiotics beyond the cells. The binding location of efflux pumps may be affected by ZDI acting as a competitive antibiotic inhibitor in this instance (Padwal *et al.*, 2014). Disrupting efflux kinetics is another potential mechanism (Nallathamby *et al.*, 2010). ZDI may terminate the proton gradient, inducing disruptions or the loss of the proton motive force (PMF) of the membrane which would weaken the driving force required for the efflux pump to function (Fig. 2) (Choi *et al.*, 2008; Dibrov *et al.*, 2002; Padwal *et al.*, 2014).

1.6 Aims and Motivation of the Study

IONPs exhibit remarkable antimicrobial properties opening a door to be a potential antimicrobial agent. Development of enhanced antimicrobial agent (transition metal-doped-IONPs) could provide significant advantages in the treatment of AMR by reducing adverse effects. Previously, bare IONPs and different metal-doped-IONPs exhibited enhanced antimicrobial activity by disrupting cell membrane integrity, reducing antimicrobial gene expression, inhibiting DNA replication and enzymes, and generating ROS as well as hemocompatibility. Therefore, ZDI could also have potential antimicrobial activities in resistant bacteria. As gram-positive and gram-negative bacteria are continuously gaining resistance throughout the years, the current study aimed to investigate the antimicrobial activity and hemocompatibility of ZDI.

1.7 Hypothesis and Objectives

Previously it was seen that the metal-doped-IONPs presented a clear antimicrobial activity against different bacteria. Upon preliminary findings it was hypothesized that the ZDI synthesized in the CP method will be effective as antimicrobial agent against gram- positive (*B. cereus, B. subtilis*) and gram-negative bacteria (*Salmoella paratyphi, K. pneumoniae)* and will enhance the efficiency of these resistant antibiotics. Additionally, it will show hemocompatibility

against red blood cells and will produce a potential combination with antimicrobial drugs. The aforementioned goals will deal with these claims:

1. To synthesize and characterize ZDI.
2. To examine potential antimicrobial activities against both resistant gram-positive and gram-negative resistant bacteria.
3. To investigate the hemocompatibility of ZDI towards human RBC.

Chapter 2

2 Materials and Methods

2.1 Chemicals and Reagents

Zinc chloride ($ZnCl_2$), iron chloride ($FeCl_3$), sodium hydroxide (NaOH), Nutrient agar (NA), Mueller-Hinton agar (MHA) and Lysogeny broth (LB) were purchased from Mark Chemicals and HiMedia Laboratories Pvt. Ltd, India. Glycerol ($C_3H_8O_3$) for stocking was obtained from FUJIFILM Wako Pure Chemical Corporation, Japan. *B. cereus, B. subtilis, K. pneumoniae, S. paratyphi* were kindly provided by the Department of Mathematics and Natural Sciences Laboratory of BRAC University, Dhaka, Bangladesh.

2.2 Synthesis of Zinc-Doped-Iron Oxide Nanoparticles (ZDI)

ZDI was synthesized through previously described protocol of CP method with minor modifications (Shakil et al., 2020). The reaction as follows –

$$ZnCl_2 + 2FeCl_3 + 8NaOH \rightarrow ZnFe_2O_4 + 8NaCl + 4H_2O \quad (1)$$

Two separate aqueous solutions of $FeCl_3$ (Mark, India) and $ZnCl_2$ (Mark, India) of analytical grade were mixed carefully in the required molar ratio. Under the rigorous hot plate magnetic stirring, 8 M NaOH (Mark, India) solution was added drop-wise and the pH of the solution was maintained between 7-7.4 ranges. To control the pH, an extra NaOH solution was added as required. The supernatant was decanted after allowing the colloid to settle down. By using a centrifugation method at 15000 rpm for 20 min solvents were extracted by centrifugation machine (Tomy MX-307). The process was repeated 10 times until the completion of extraction. To obtain the final product the precipitate was annealed for 72 h at 90 °C. The flow diagram of the CP synthesis method is attached below (Figure 3):

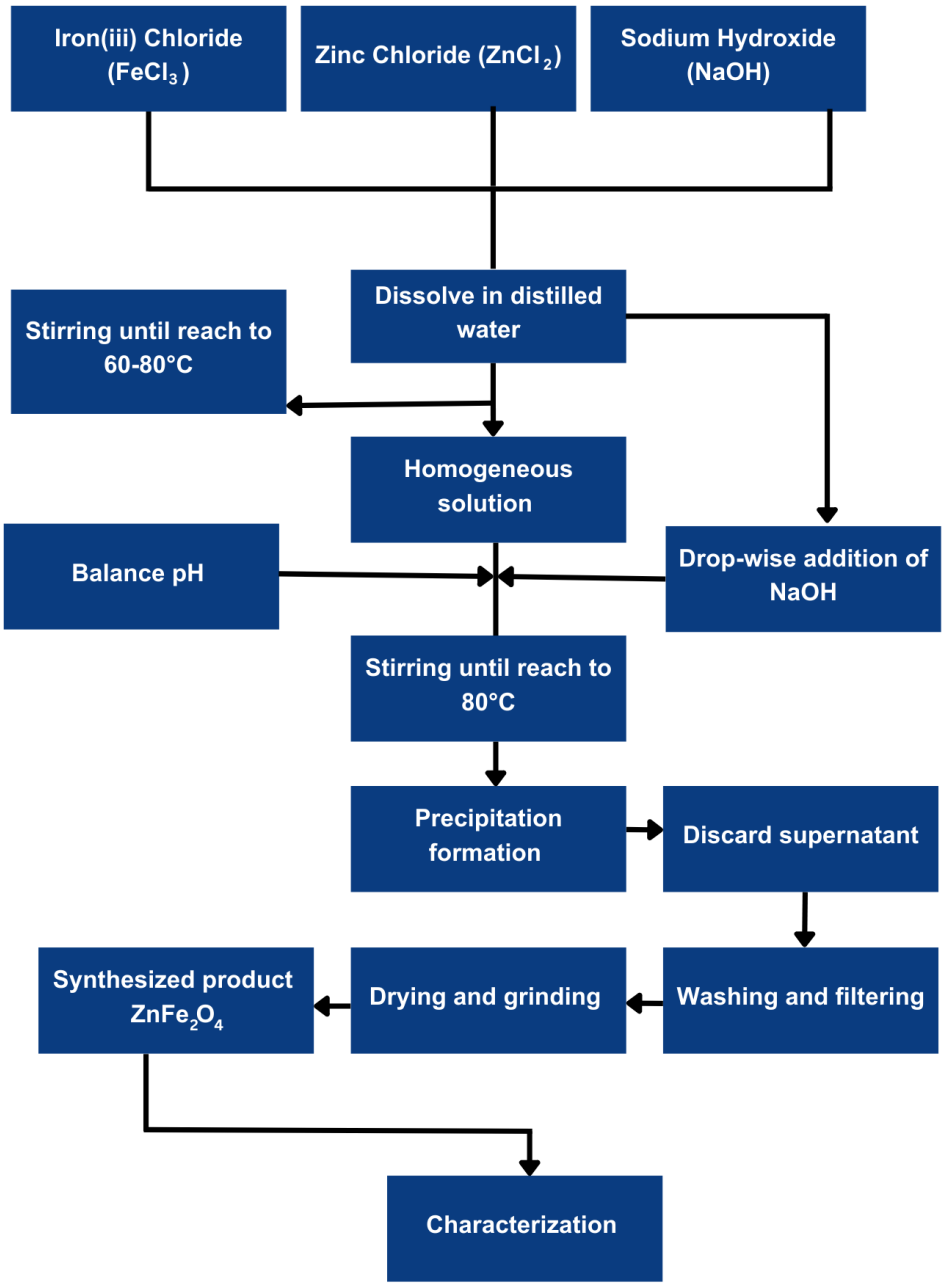

Figure 3: Flow diagram of CP synthesis method of ZDI. ZDI: Zinc-doped-iron oxide nanoparticles. CP: Co-precipitation

2.3. Characterization

2.3.1 Fourier-Transform Infrared Spectroscopy (FTIR)

FTIR is a technique which is used to acquire the infrared spectrum of absorption, emission, and photoconductivity of solid, liquid, and gas. It is utilized to find various functional groups that are present in nanoparticles. Using a Cary 630 FTIR instrument, the surface functional group analysis of the ZDI samples was carried out. Software called Spectraglyph was used to process the obtained spectra (Software-Entwicklung, Oberstdorf, Germany).

2.4. Glycerol Stock Preparation

A single colony from overnight culture was inoculated into 5 mL LB and incubated at 37°C for 24h with moderate shaking. Then, 500µL of liquid bacterial culture was added into 1.5mL micro-centrifuge tubes. 500µL pre-sterilized, 50% Glycerol was poured directly into the liquid bacterial culture. The final proportions of glycerol stock were 50% bacteria and 50% diluted glycerol. Each vial was kept for incubation at 37°C for 1-2 h and stored at −20°C.

2.4.1 Reviving Glycerol-Recovered Cultures

A loop full of organisms was scraped up and streaked onto selective agar plates and incubated at 37°C overnight. The bacterial scraping was not be thawed. 1.5mL micro-centrifuge tubes were kept on ice until the completion of the tests. Samples were pulled out of the freezer only when necessary (Hoque *et al*., 2016).

2.4.2 Preparation of Sample Disk with Test Samples

Sterile metrical filter paper disks (Whatman® antibiotic assay disk, 6 mm diameter) and antibiotic disks (MT and AMX, 5 and 30µg, respectively) were taken in a petri dish and soaked with different concentrations (5, 10, 15 mg/mL) of ZDI. The disks were kept to dry properly for several minutes.

2.5. Antimicrobial Tests

Bacterial strains used to determine the antimicrobial potential of ZDI, and ZDI combined with antibiotics (AMX, MT) include gram-positive bacteria (i.e., *B. cereus, B. subtilis), and* gram-

negative bacteria (i.e., *K. pneumoniae, S. paratyphi*). The antimicrobial activities were evaluated in terms of their ZOI in millimeter (mm) scale, minimum inhibitory concentration (MIC).

2.5.1 Kirby-Bauer Disk Diffusion Method

The antimicrobial activity of ZDI was determined by Kirby-Bauer Disk Diffusion method (Bauer et al., 1966). The Kirby-Bauer disk diffusion method is performed to determine the antimicrobial activities of antimicrobial agents against bacterial strains and the results are categorized as susceptible, intermediate, or resistant according to Clinical and Laboratory Standards Institute (CLSI) guidelines (Humphries et al., 2018). For the procedure, 35mL MHA was poured into large plate (150mm diameter). At first, test tubes with 10 mL saline water (.9% NaCl) were inoculated with a single colony of overnight culture and vortexed properly. The turbidity of the inoculums was adjusted to 0.5 McFarland standards which is equivalent to 1-2 $\times 10^8$ CFU/mL. Then the sterile cotton swabs were dipped into the test tubes and pressed against their walls to scrape off the excess inoculums. With that, a bacterial lawn was prepared and disks were placed. Plates were kept for incubation at 37˚C for 24 h. Then the results were observed by measuring ZOI in millimeters (mm).

2.5.2 Well Diffusion and Determination of ZOI

Well diffusion method was also performed for a better comprehension of its liquid form against both gram-positive and gram-negative bacteria via previous protocol with minor modifications(Bauer *et al*., 1966). Briefly, instead of disks, well (6 mm diameter) was punctured onto agar media. 150 µL of different concentrations of ZDI (i.e., 5, 10, 15 mg/mL) and antibiotic solutions (MT and AMX, 5 and 30µg/mL, respectively) were poured into the wells. The plates were incubated at 37˚C overnight for optimum growth. The antimicrobial activity of ZDI and ZDI combined with antibiotics were determined by measuring ZOI. A millimeter scale was used to measure the diameter of the ZOI at 24 h.

2.5.3 Determination of the MIC and IC_{50}

The lowest amount of antimicrobial agent required to inhibit the growth of a bacterial strain is considered as MIC value and the concentration of antimicrobial agent needed to inhibit biological process or response by 50% is known as half maximal inhibitory concentration (IC_{50}). The MIC value of ZDI was determined via previous protocol (Mondal *et al.*, 2017). In brief, 10

μL of the overnight bacterial cultures were mixed with 990 μL of freshly prepared LB broth and incubated at 37 °C and 120 rpm for 4 h. Then, 200μL of different concentrations of ZDI and antibiotics were added to the 1×10^8 CFU/mL bacterial culture and incubated overnight at 37 °C and 120 rpm. The optical density of respective bacterial strains was determined at 600 nm to measure the MIC values of the ZDI and antibiotics. The experiment was conducted several times, and the data were reported as the mean of several replications (n = 3) and standard deviations. The percentage of cell inhibition and cell viability were determined by applying Eq. (2-3).

Inhibition % = $\{1 - (A_{sample} - A_{sample}\ blank)/ A_{control} - A_{control}\ blank\} \times 100$ (2)

Cell viability % = (100- Cell inhibition %) (3)

2.6 Hemocompatibility Test

2.6.1 *In Vitro* Hemolysis Assay

The hemocompatibility of ZOI in O^+ve blood group from both genders (non-smoker) was investigated against human RBCs by following this protocol (Aktanova *et al.*, 2021). However, slight modifications were made. Briefly, 10 mL of human blood was drawn via venipuncture method from a 20–30 year old healthy person and preserved in a tube with 10% EDTA as an anticoagulant. To separate RBCs from serum, the blood samples were centrifuged at 5000 rpm for 5 minutes at room temperature. After aspirating the serum, precipitated RBCs were resuspended in 5 mL of phosphate-buffered saline (PBS, pH 7.4), and the mixture was centrifuged at 5000 rpm for 5 minutes. Then the RBCs were washed twice with 5 mL phosphate-buffered saline (pH 7.4) solution at 5000 rpm for 5 min. Thereafter, 35 mL of PBS was used to prepare the RBC suspension. After that, 200μL of various nanoparticles concentrations were added to the RBC solution (1 mL), and the mixture was incubated for an hour at 37 °C with moderate shaking. Combinations of RBC and nanoparticles were centrifuged for 5 minutes at 5000 rpm. After gathering the supernatant, the absorbance at 570 nm was calculated. In this experiment, RBCs treated with PBS and Triton X-100 served as the negative and positive controls, respectively. The level of lysis was determined for each replicate after the entire experiment was run three times with the following Eq. (4)-

$$\text{Hemolysis (\%)} = 100 \times (\text{Abs} - \text{Ab0}) / ((\text{Abs100} - \text{Abs0}))) \quad (4)$$

Abs—absorption index for the test sample;

Ab0—absorbance index for negative control (PBS buffer);

Abs100—Absorption index for positive control (Triton X-100) (Aktanova et al., 2021).

2.7 Statistical Analysis

Each test were performed in triplicate, and the mean ± standard deviation (SD) was measured via GraphPad Prism (version 7.03). The results of disk and well diffusion test was analyzed using one-way ANOVA coupled with Tukey's multiple comparisons test.

Chapter 3

3 Results

3.1 FTIR Analysis

Analysis was done on the FTIR spectra of ZDI (Figure 4). Metal oxides (M-O) are visible as peaks at about 536 cm^{-1} and 435 cm^{-1}, where M represents Fe and Zn (Jing & Wu, 2004; Liu et al., 2009). The existence of the O-H group is indicated by the widest absorption peak, which was seen at approximately 3400 cm^{-1}. The O-H group is present as a result of the atmosphere's water and moisture absorption. Moreover, samples of ZDI have a peak at 1181 cm^{-1}. This peak is caused by the existence of the C-O group, which is brought on by samples of the environment absorbing CO_2. ZDI exhibits minimal CO_2 and moisture absorption. This alteration may be the result of variations in the humidity of the air during sample preparation (Darezereshki, 2011; Sultan *et al.*, 2021).

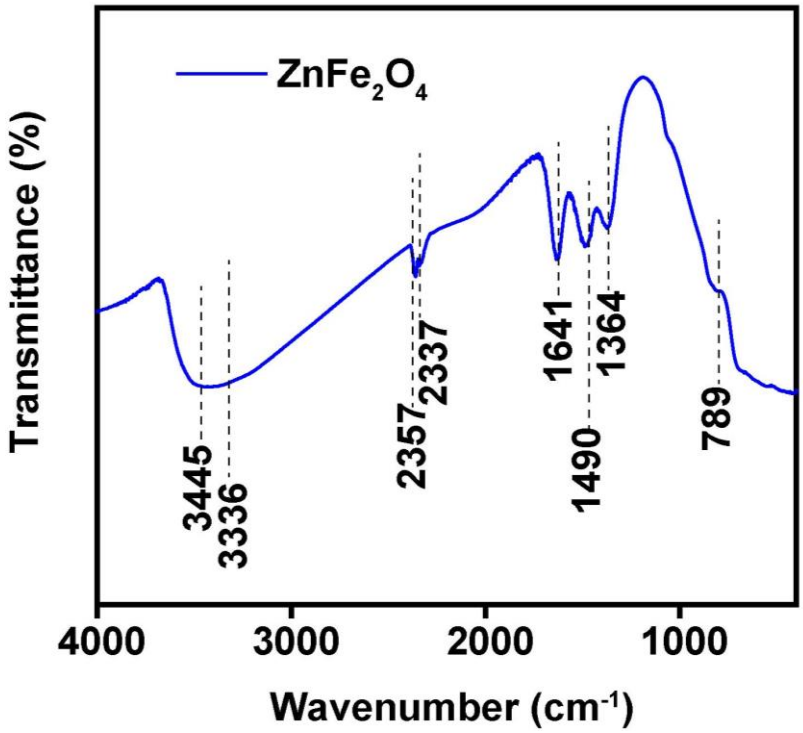

Figure 4: FTIR spectrum of synthesized ZDI. Fe-O, Zn-O, O-H and C-O stretching peaks were visible at 536, 435, 3400, 1181 cm^{-1}, respectively.

3.2 Antimicrobial Test

Figure5.1.1, 5.1.2, 5.1.3, 5.1.4 and 5.2.1, 5.2.2, 5.2.3, 5.2.4 show the results of antimicrobial properties of the disk and well diffusion assay of ZDI and ZDI combined with antibiotics against all the tested gram-positive and gram-negative bacteria.

The maximum ZOI was produced against gram-positive bacteria *B. subtilis* (20 mm) at 15 mg/mL concentration in well diffusion (Figure 6.2). The respective inhibition zone diameters of the prepared samples against all the tested bacterial strains are summarized in figure6.1 and 6.2. Based on the disk and well diffusion experiment, the following bacteria had the highest sensitivity to ZDI and ZDI combined with antibiotics: *B. subtilis* > *B. cereus* > *K. pneumoniae* > *S. paratyphi*. However, Tukey's multiple comparison tests showed statistically no significant differences between ZDI and ZDI combined with antibiotic tests. The experiments were carried out thrice to obtain the values of the zone of inhibition.

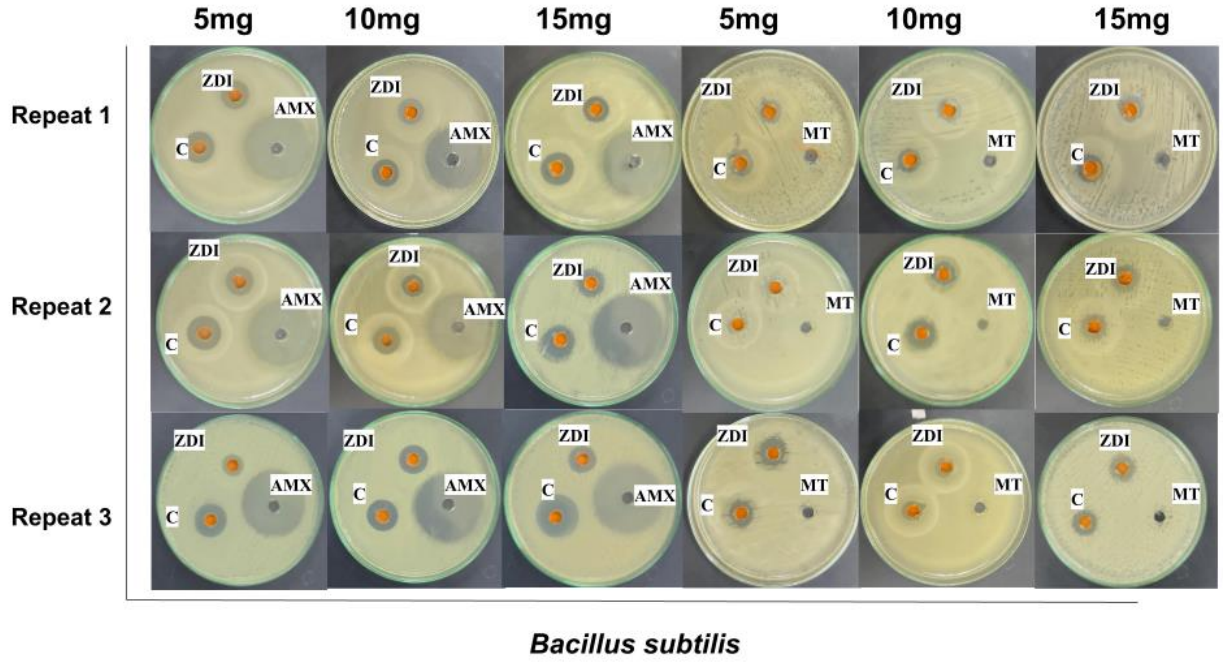

Figure 5.1.1: Photograph of Kirby-Bauer disk diffusion method on *B. subtilis*. ZDI: Zinc-doped-iron oxide; AMX: Amoxicillin MT: Metronidazol.

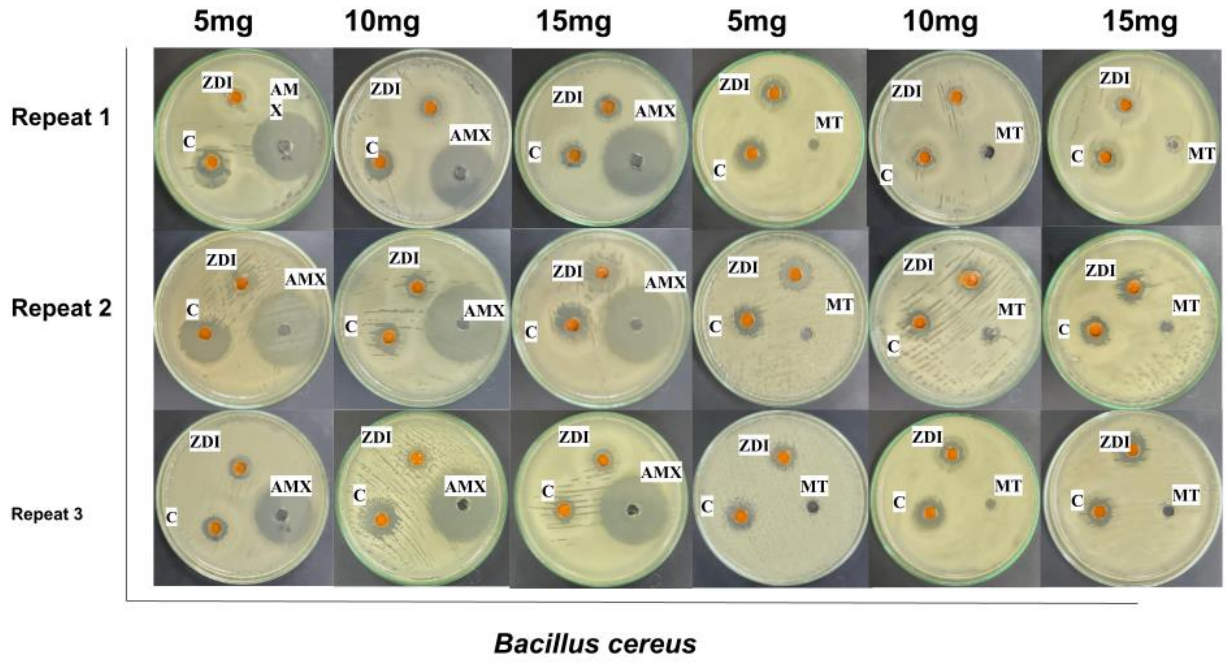

Figure 5.1.2: Photograph of Kirby-Bauer disk diffusion method on *B. cereus*. ZDI: Zinc-doped-iron oxide; AMX: Amoxicillin MT: Metronidazol.

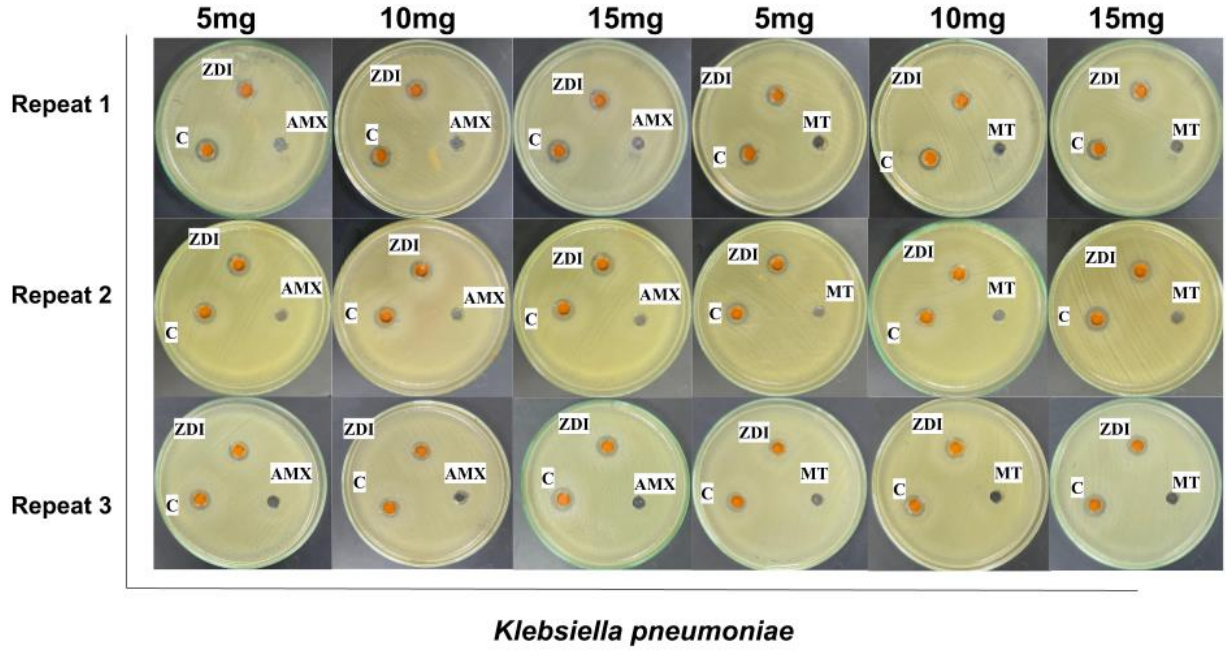

Figure 5.1.3: Photograph of Kirby-Bauer disk diffusion method on *K. pneumonia*. ZDI: Zinc-doped-iron oxide; AMX: Amoxicillin MT: Metronidazol.

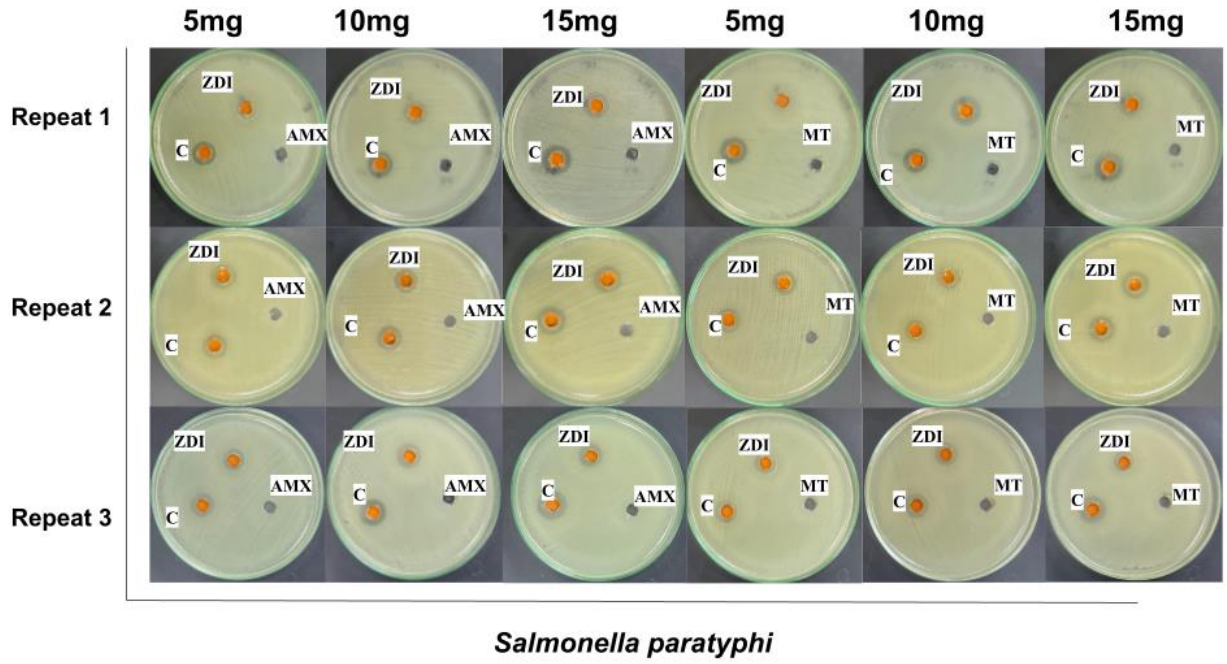

Figure 5.1.4: Photograph of Kirby-Bauer disk diffusion method on *S. paratyphi*. ZDI: Zinc-doped-iron oxide; AMX: Amoxicillin MT: Metronidazol.

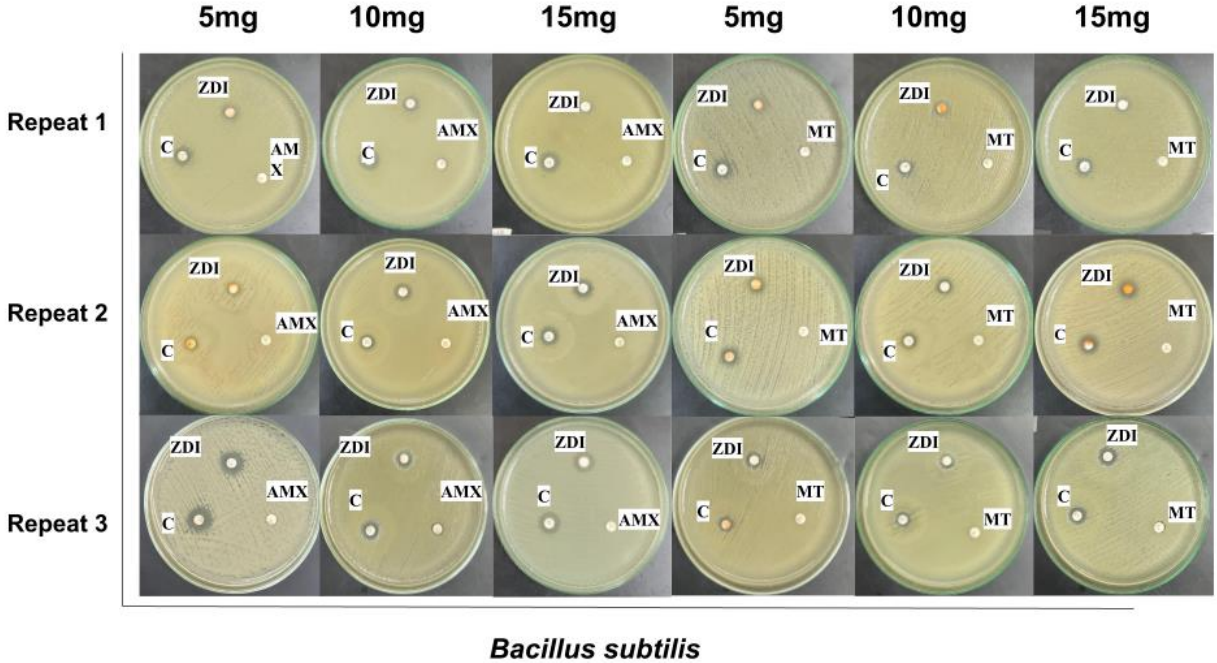

Figure 5.2.1: Photograph of Kirby-Bauer disk diffusion method on *B. subtilis*. ZDI: Zinc-doped-iron oxide; AMX: Amoxicillin MT: Metronidazol.

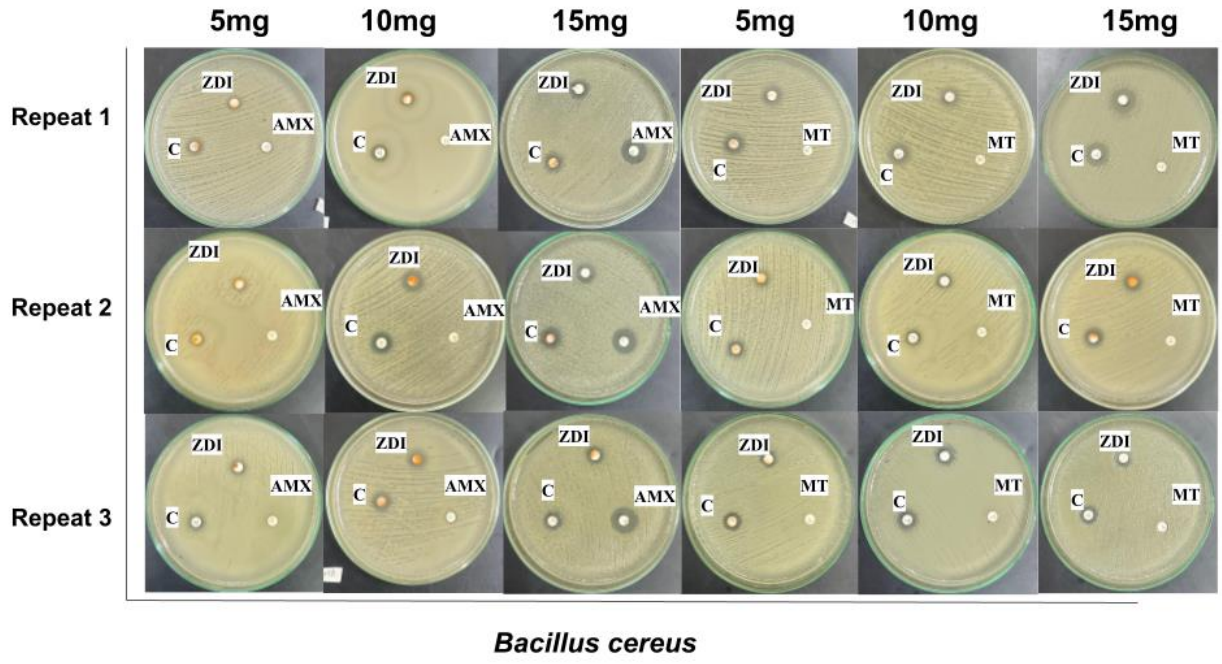

Figure 5.2.2: Photograph of Kirby-Bauer disk diffusion method on *B. cereus*. ZDI: Zinc-doped-iron oxide; AMX: Amoxicillin MT: Metronidazol.

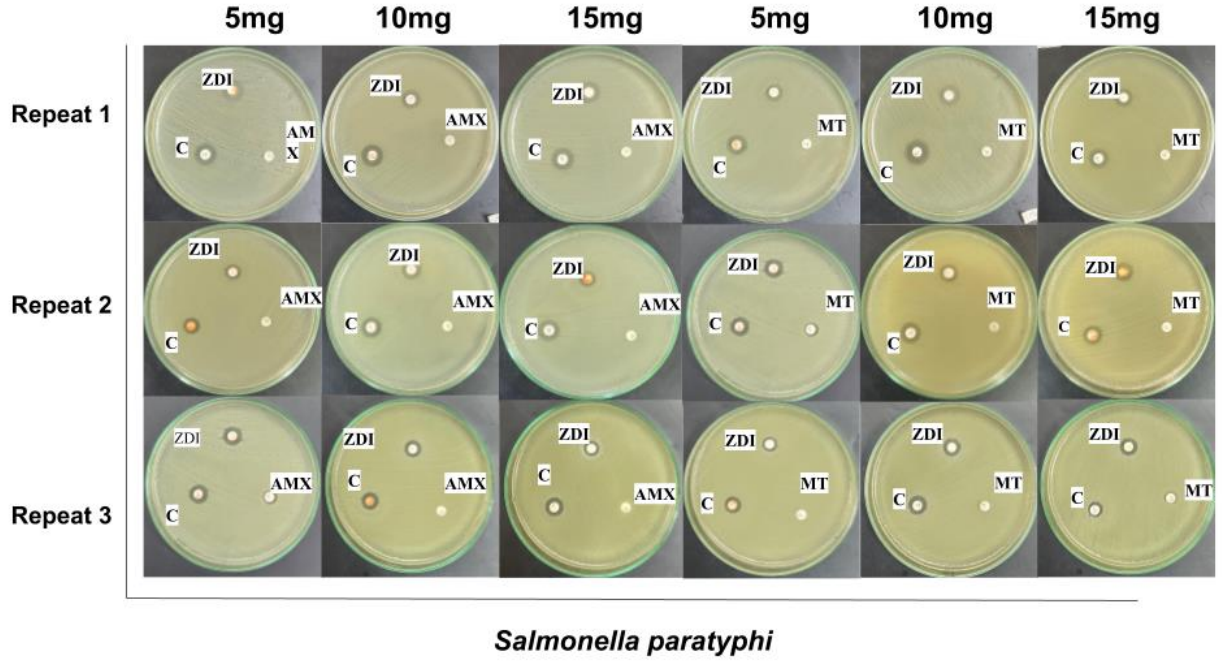

Figure 5.2.3: Photograph of Kirby-Bauer disk diffusion method on *S. paratyphi*. ZDI: Zinc-doped-iron oxide; AMX: Amoxicillin MT: Metronidazol.

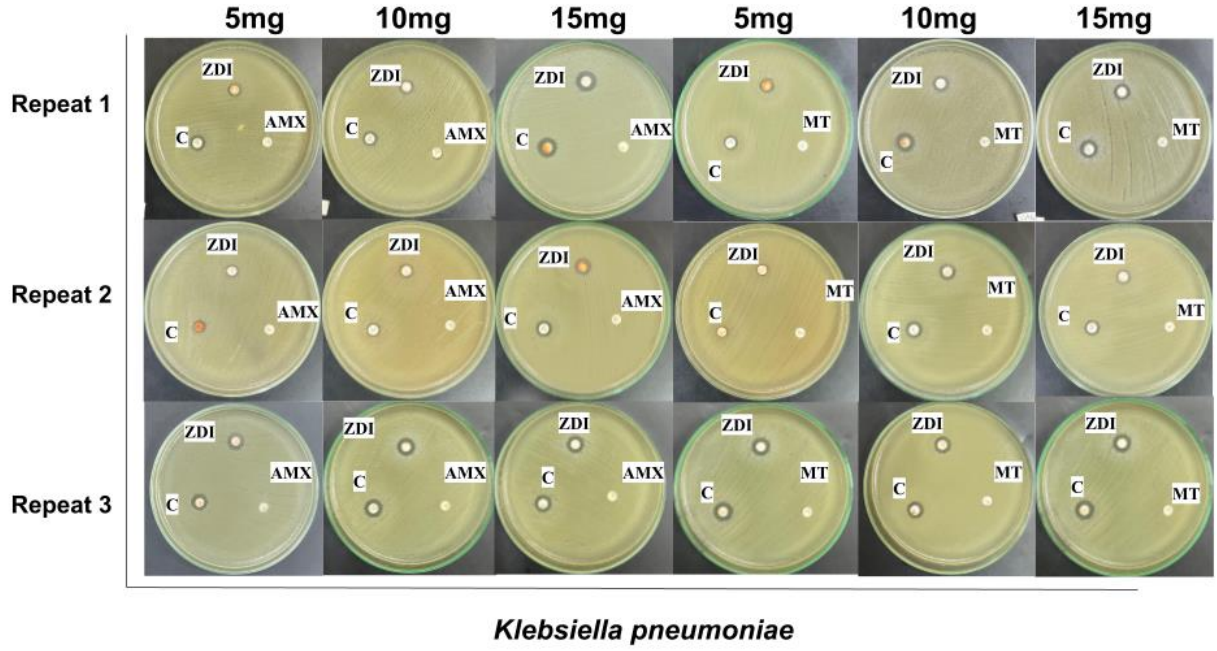

Figure 5.2.4: Photograph of Kirby-Bauer disk diffusion method on *K. pneumoniae*.ZDI: Zinc-doped-iron oxide; AMX: Amoxicillin MT: Metronidazol.

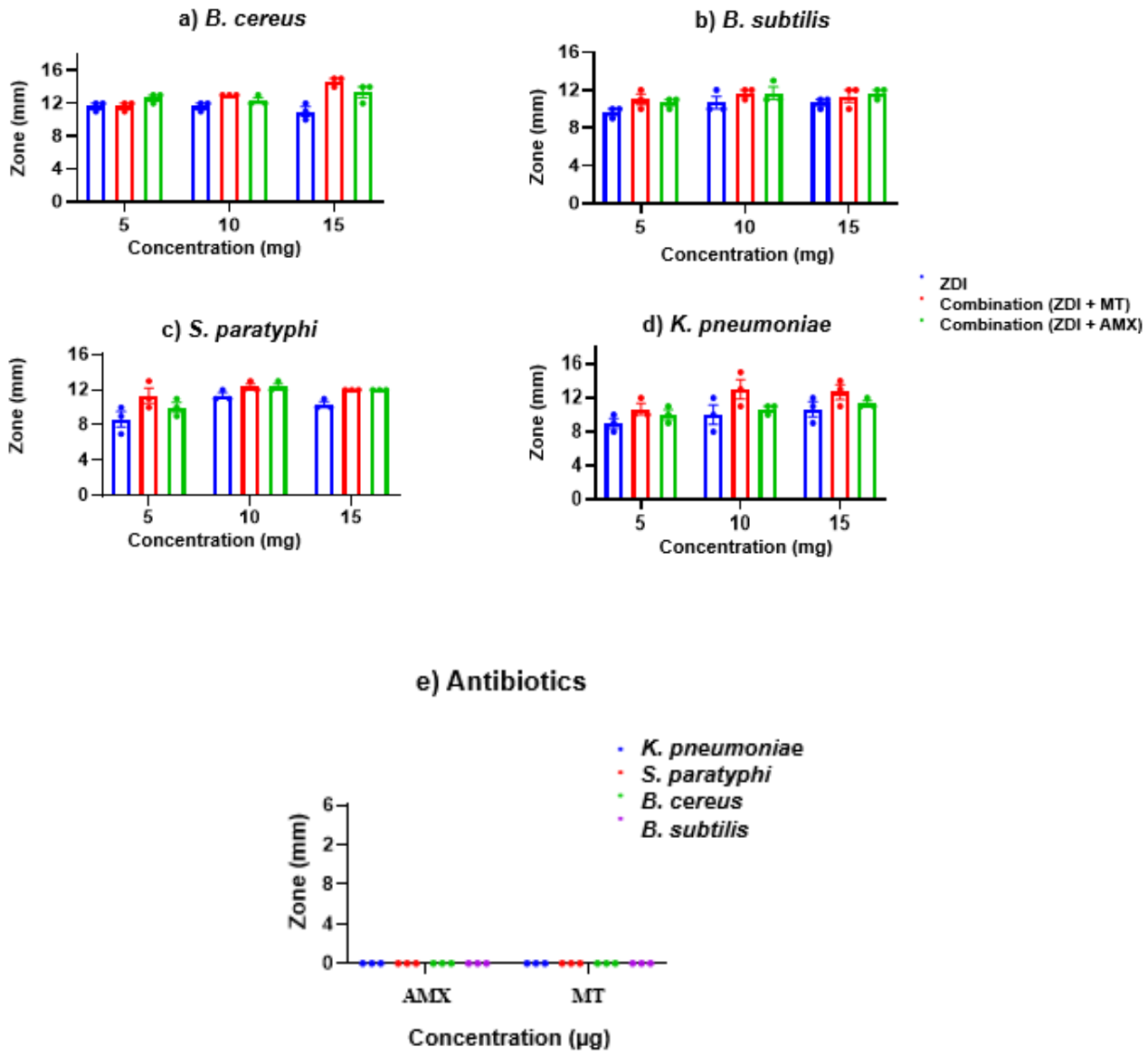

Figure 6.1: Estimated ZOI after treatment of pathogenic bacteria with various concentrations of ZDI by Kirby-Bauer disk diffusion method. a) ZOI of *B. cereus* was around 12-14 mm b) ZOI of *B. subtilis* was around 10-12 mm c) ZOI of *S. paratyphi* is around 8-12 mm d) ZOI of *K. pneumoniae* was around 9-12 mm. Among all, ZDI had demonstrated the highest ZOI (14 mm) against *B. cereus* at 15 mg concentration.

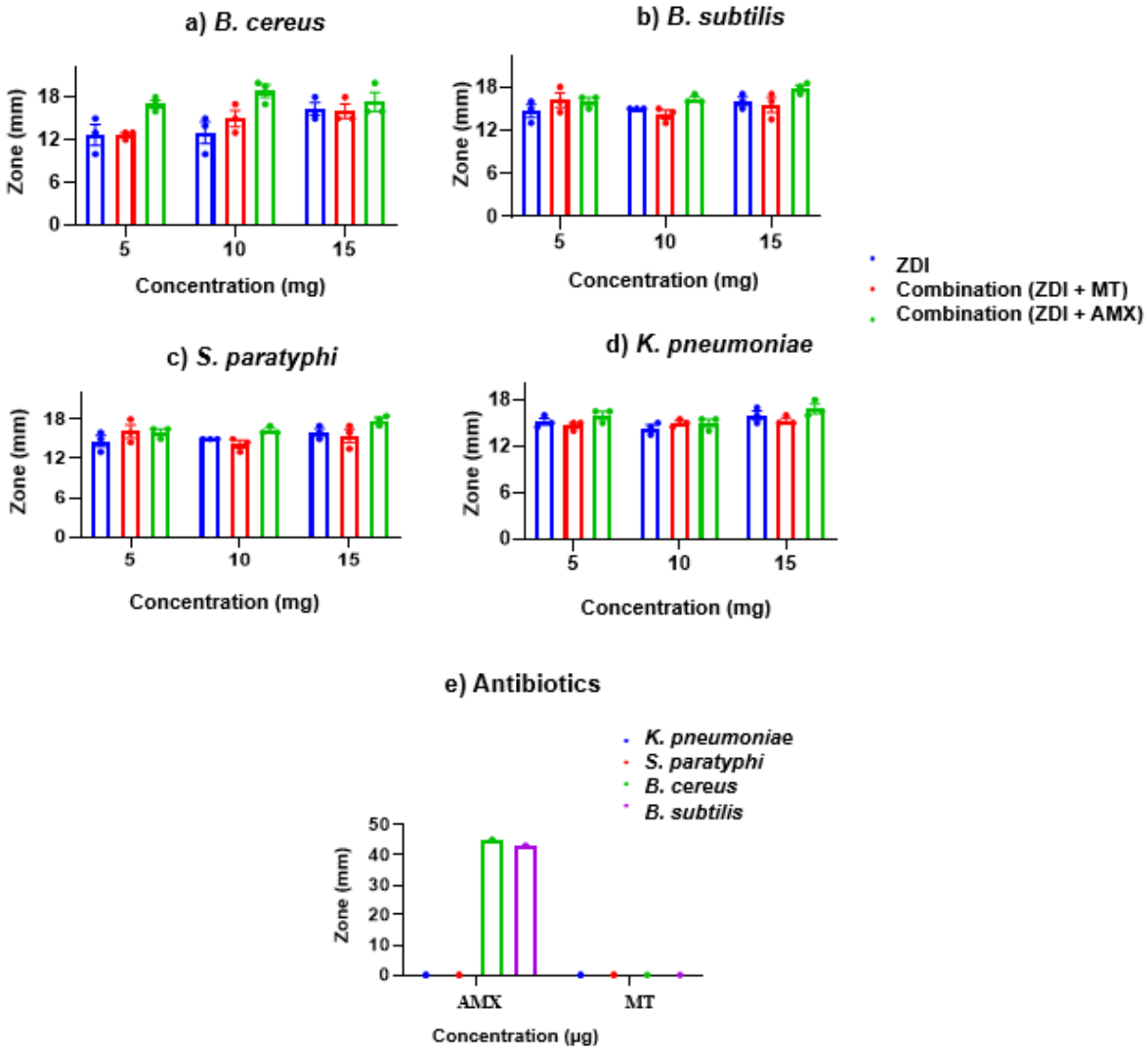

Figure 6.2: Estimated ZOI after treatment of pathogenic bacteria with various concentrations of ZDI by well diffusion method. a) ZOI of *B. cereus* is around 12-18 mm b) ZOI of *B. subtilis* was around 14-18 mm c) ZOI of *S. paratyphi* was around 13-17 mm d) ZOI of *K. pneumoniae* was around 13-17 mm. Among all, ZDI had demonstrated the highest ZOI (18 mm) against *B. cereus and B. subtilis* at 15 mg concentration. ZDI had demonstrated the highest ZOI (18mm) against *B. subtilis* at 15 mg concentration. AMX and MT had served as positive and negative control. AMX: Amoxicillin MT: Metronidazol.

3.3 MIC and IC_{50}

The MIC value of ZDI, and antibiotics (AMX, MT) were determined against 1×10^8 CFU/mL for each bacterium. The MIC test revealed the mean MIC of *B. cereus*, *B. subtilis*, *K. pneumonia*, *S. paratyphi* which are 0.024, 0.017, 0.041 and 0.331 µM/mL, respectively. The MIC values of the antibiotics (i.e. AMX, MT) are given in table 3. IC_{50} values were determined within 0.0-

414.8 µM/mL concentration to understand the effect of ZDI on cell viability (Figure 7). The lowest IC_{50} was determined against *B. subtilis* at .11 µM/mL concentration.

Table 3: Minimum inhibitory concentration of ZDI, AMX, MT on bacteria

Bacteria	**MIC**		
	ZDI (µM/mL)	**AMX (µM/mL)**	**MT (µM/mL)**
B. cereus	0.024	0.004	1.037
B. subtilis	0.017	0.004	0.414
K. pneumoniae	0.041	1.037	1.037
S.paratyphi	0.331	1.037	3.111

MIC: Minimum inhibitory concentration; ZDI: Zinc-doped-iron oxide nanoparticles; AMX: Amoxicillin; MT: Metronidazol

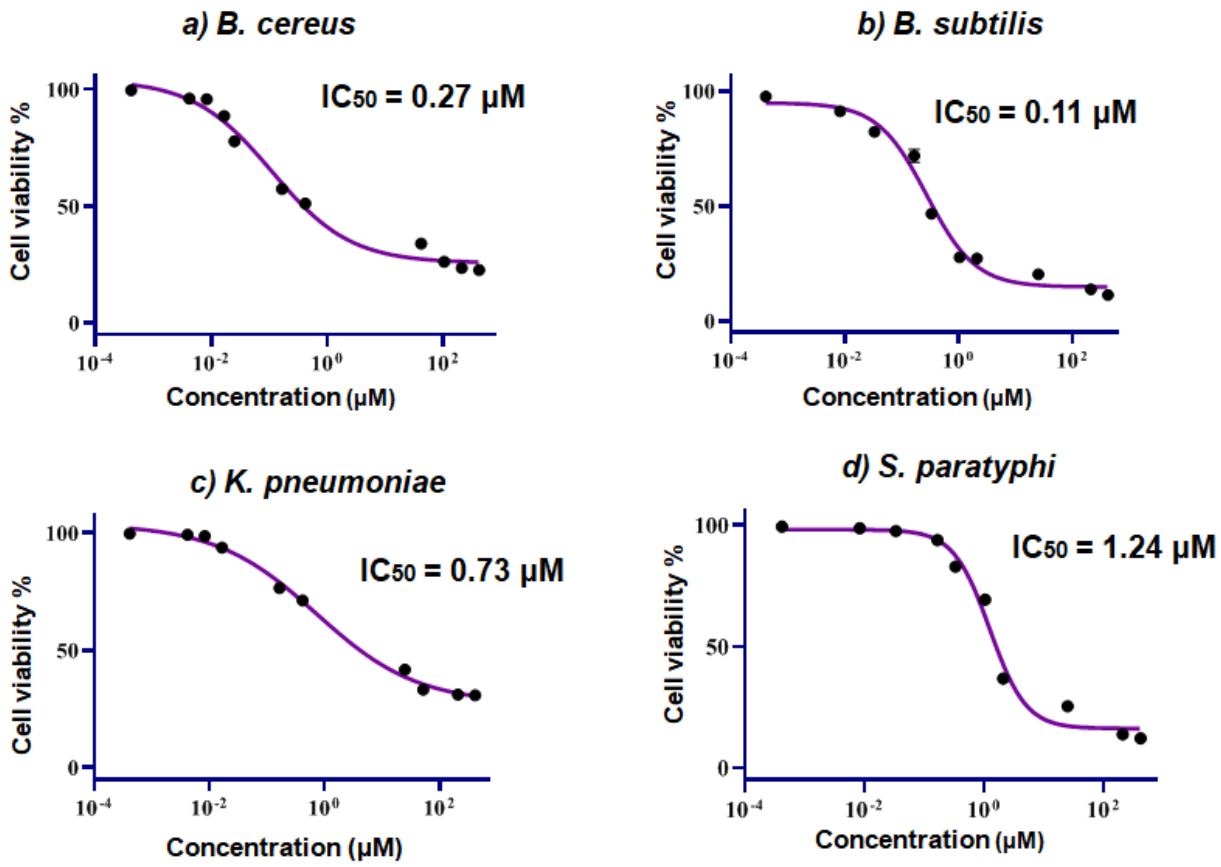

Figure 7: Half maximal inhibitory concentration (IC_{50}) of ZDI on bacteria. a) IC_{50} of *B. cereus* is 0.27 µM b) IC_{50} of *B. subtilis* is 0.11 µM c) IC_{50} of *S. paratyphi* is 0.73 µM d) IC_{50} of *K. pneumoniae* is 1.24 Mm**.** The lowest IC_{50} demonstrated by *B. subtilis* at .11 µM.

3.4 *In vitro* Hemolytic Property of ZDI

A representative photograph of the degree of hemolysis induced by ZDI when exposed to human blood (O^+ve), for 4 h of incubation is shown in figure 8. The percentage of lysis of the cells increased as a function of increasing mass concentration of particles in the blood. ZDI concentrations below the threshold (10 mg) did not result in any significant hemolysis. Concentrations of ZDI at or above (20 mg/mL) triggered higher levels of hemolysis, exceeding upto15% hemolysis in both genders, as shown in figure 8.1.

As per the criterion in the ASTM E2524-08 standard (Dobrovolskaia et al., 2008), the percentage of hemolysis > 5% indicates the following test material causes damage to RBCs; this criterion was exceeded at the particle concentration of 20 mg/mL for both male and female.

Experiments consisting of negative control and positive control (Triton X-100 and PBS, respectively), confirmed the efficacy of the hemolysis assay.

Figure 8: Blood group-dependent *in vitro* hemolysis assay. A photograph of hemolysis assay of ZDI-treated RBC.PBS and Triton X-100 lysed blood cells served as NC and PC, respectively. ZDI: Zinc-dope-iron oxide nanoparticles, RBC: Red blood cells, PBS: Phosphate Buffer Solution.

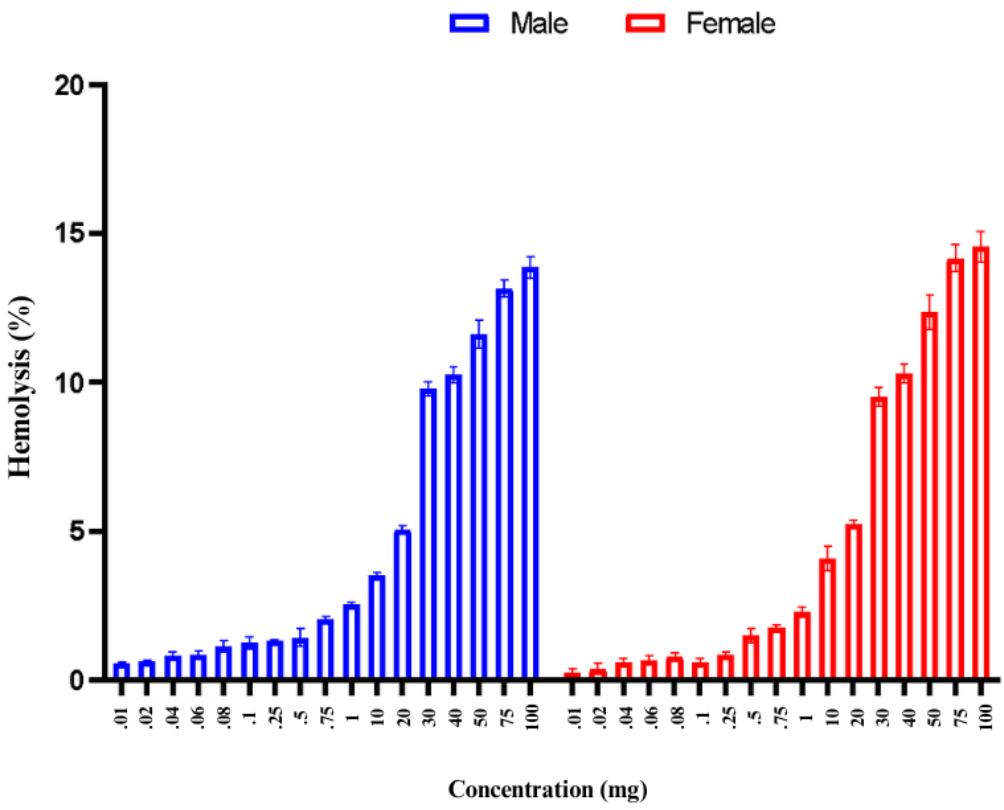

Figure 8.1: Hemocompatibility of ZDI. Percentage of lysed RBC of treated with ZDI from both healthy male and female. The values presented in the graph are mean of triplicate. ZDI: Zinc-doped-iron oxide nanoparticles; RBC: Red blood cells.

Chapter 4

4 Discussions

In this study, ZDI was synthesized via CP method. CP is a sequential chemical process in which a metallo-organic precursor undergoes nucleation, then aggregation or Ostwald ripening to generate metal oxides (Arulmurugan *et al*., 2005). It is one of the most extensively utilized procedures due to its high yield and simplicity in manufacturing high purity ultrafine magnetic nanoparticles specially ferrites (Chia *et al*., 2010; Vinosha *et al*., 2021) . It is a simple and low-cost method that results in materials with high crystallinity, requires low temperature, homogeneity, and good textural properties (Chand *et al.*, 2017; Vinosha et al., 2021). The CP method is identical to the precipitation method. The distinction lies in the use of more than one soluble component to precipitate in one solution at the same time. This is a good method for achieving solid dispersion (Yaqoob *et al*., 2021). Moreover, CP approach has the benefit of producing crystalline sizes in the limited range as compared to other synthesis procedures, depending on the precipitating agent used during the reaction. When direct precipitation cannot separate the required metallic species due to its low concentration in the sample solution, CP is utilized (Bulut *et al*., 2008). The size, shape, and magnetic characteristics of the nanoparticles may be adjusted by modifying the experimental parameters e.g. reaction temperature and duration, reagent feeding rate and concentration, pH, drying temperature, and so on (Prabhakaran *et al*., 2017).

The main disadvantages of CP techniques included agglomeration, poor crystallinity and particle size distribution, and the need for pH control (Houshiar et al., 2014; Zahraei *et al.*, 2015). The difficulty of scaling up for mass production is one of the key limitations of the traditional CP synthesis method. The greater the reaction volume, the more complicated to achieve homogeneity (Li *et al*., 2008). Additionally, gas, such as nitrogen, can be blown over the sample to assist preserve the pH and prevent the components from oxidizing (Liang *et al*., 2007). Traditional CP procedures may generate IONPs with broader size distribution and batch-to-batch variability in IONPs size, crystallinity, morphology, and other physicochemical features due to a lack of control over mixing and other factors (Ahrberg *et al.*, 2018).

In FTIR analysis, the functional groups and vibrational studies confirmed the doping of ZDI. The existence of C-O and O-H groups indicated the minimal CO_2, water and moisture absorption and this alteration occurred due to variations in the humidity of the air during sample preparation (Darezereshki, 2011; Sultan *et al*., 2021).

In the antimicrobial susceptibility tests, the basic principle of the disk diffusion assay is that the paper disks absorb water from the agar, after which the impregnated ZDI start diffusing into the agar and, if they exhibit antibacterial characteristics, inhibit bacterial growth around the disk. As a result, the size of the inhibition zone formed around the disk provided an indirect indication of the impregnated material's antimicrobial activities against the tested microorganisms. Well diffusion also followed the similar principle of diffusion. After 24 hours of incubation, the ZOI was observed around the well and disks loaded with the ZDI and ZDI combined with antibiotics and the presence of the inhibition zone demonstrate the antimicrobial activity of the respective ZDI concentration. Moreover, MIC and IC_{50} also determined the lowest concentration required for ZDI to inhibit the bacteria and concentration required to inhibit 50% growth.

Gram-positive bacteria were more susceptible to ZDI than gram-negative bacteria. The possible reason could be due to their cell wall and cell membrane composition. Gram-positive bacteria lack an outer membrane and rely only on the peptidoglycan layer, which is a weak permeability barrier (Bhattacharya & Neogi, 2018). While gram-negative bacteria have chemically complicated cell walls with an outer membrane made of proteins, phospholipids, and lipopolysaccharides and a thin peptidoglycan layer beneath (Aruguete & Hochella, 2010). Moreover, lipopolysaccharides are reported to be present in the outer membrane of gram-negative bacteria, which increases the net negative charge of the cell membrane (Hajipour *et al*., 2012),and prevents the penetration of negatively charged free radicals and makes the cell membrane impermeable to lipophilic solutes. As a result, it was asserted that gram-negative bacteria were less sensitive to nanoparticles (Ismail *et al.*, 2015). Another explanation could be the size, shape, and surface charge of the ZDI made them more suited to interact with gram-positive bacteria, although further study was required(Jiang *et al*., 2020).

In addition to antimicrobial testing, we further investigated the impact of ZDI on human RBC. Nanoparticles have been identified to trigger persistent biochemical and morphological

alterations (erythrocyte membrane disruption), adversely affecting red blood cell functions and leading to hemolysis (Haghniaz et al., 2021; Manaargadoo-Catin *et al.*, 2016). Mohamed *et al*. (2020) reported that, IONPs induce 75% hemolysis at 600µg/mL and 12.48 % hemolysis at 12.5 µg/mL(Mohamed *et al*., 2020). Interestingly, in our study, concentrations up to 10 mg /mL triggered < 5% hemolysis of ZDI-treated RBC in both gender. However, ≥ 5 % hemolysis was noticed at 20-100 mg/mL concentrations. Additionally, our results concurred with the findings reported by Martnez*et al*. (2019) and Haghniaz*et al.* (2021) that ZDI did not promote hemolysis at .2 mg/mL(Haghniaz *et al.*, 2021; Martínez-Rodríguez *et al*., 2019). The outcome indicated that a transition metal (zinc) might substantially enhance hemocompatibility when added to an iron oxide formulation by doping.

4.1 Limitations

Although ZDI demonstrated antimicrobial activity and hemocompatibility the current study had some limitations. All the data of MIC ad IC_{50} were not statistically evaluated. Moreover, the level of hemolysis compared to the true positive or true negative had not been investigated. One of the main challenges of using IONPs *in vivo* and *in vitro* was their toxicity and propensity to aggregate due to strong magnetic attraction, and high surface energy (Xia *et al.*, 2012). To address these issues, various types of surface modification compounds could have been utilized for the coating of IONPs such as polymers (e.g. polyvinyl alcohol (Hanusch *et al*., 2014), polyethylene glycol (Stepien *et al*., 2018)), monomers (e.g. Citrate (Nigam *et al*., 2011; Stein *et al*., 2020), Carboxylic monomer (Kandasamy *et al.*, 2018)), Silica (Rivas Rojas *et al*., 2017; Yu *et al.*, 2002), Chitosan (Bandi *et al*., 2019; Hastak *et al.*, 2018; Shakil *et al.*, 2020), antioxidants (e.g. Salicylic acid (Mikhnavets *et al.*, 2022), Citric (Wang *et al.*, 2018), Ascorbic (Taei *et al.*, 2016), Gallic acid (Correcher *et al*., 2021; Shah *et al.*, 2017)), surfactant (e.g. Oleic acid (Ika O. Wulandari, 2019), Stearic acid (Jaishankar *et al.*, 2019) to increase the stability of IONPs (Laurent *et al.*, 2008; Mohammadi *et al.*, 2018; Nosrati *et al.*, 2017). Moreover, the experiments were conducted in a short period of time. Required reagents were not received on time thus the workflow was hampered.

4.2 Conclusions and future directions

ZDI was synthesized by the CP method and FTIR confirmed the functional groups of metal oxides (Fe-O, Zn-O) present in ZDI around 536, and 435 cm−1, respectively. Among all the bacteria, gram-positive bacteria exhibited the most sensitivity against ZDI. In disk and well diffusion, gram-positive bacteria (B. subtilis and B. cereus) demonstrated the highest ZOI (18mm) against ZDI. Bacillus subtilis also demonstrated the lowest MIC (0.017 µM/mL) and IC50 (0.11 µM/mL) against ZDI suggesting that the gram-positive bacteria were more sensitive towards ZDI and the possible reason could be the composition of cell wall and cell membrane structure of gram-positive and gram-negative bacteria. ZDI also demonstrated excellent hemocompatibility against RBC concentration lower than 10 mg/mL demonstrating ≤5 % hemolysis in both genders. However, the concentration at or above 20% demonstrated ≥5% hemolysis. It can be stated that doping Zinc can enhance the hemocompatibility of IONPs. Additionally, to confirm the composition regarding shape and size XRD, TEM and DSL could be performed. Moreover, to understand the anti-cancer activity and anti-biofilm activity and antibiotics further tests are recommended. Finally, investigation of the combined effect of ZDI and antibiotics using fractional inhibitory concentration can provide a conclusive result regarding cell death, concentrations, mechanism of action of antimicrobial activity, respectively.

Chapter 5

5 References

Abdel Maksoud, M. I. A., El-Sayyad, G. S., El-Bastawisy, H. S., & Fathy, R. M. (2021, Aug 16). Antibacterial and antibiofilm activities of silver-decorated zinc ferrite nanoparticles synthesized by a gamma irradiation-coupled sol-gel method against some pathogenic bacteria from medical operating room surfaces. *RSC Adv, 11*(45), 28361-28374. https://doi.org/10.1039/d1ra04785j

Adamiano, A., Wu, V. M., Carella, F., Lamura, G., Canepa, F., Tampieri, A., Iafisco, M., & Uskoković, V. (2019, May). Magnetic calcium phosphates nanocomposites for the intracellular hyperthermia of cancers of bone and brain. *Nanomedicine (Lond), 14*(10), 1267-1289. https://doi.org/10.2217/nnm-2018-0372

Ahghari, M. R., Amiri-khamakani, Z., & Maleki, A. (2023, 2023/01/18). Synthesis and characterization of Se doped Fe3O4 nanoparticles for catalytic and biological properties. *Scientific Reports, 13*(1), 1007. https://doi.org/10.1038/s41598-023-28284-x

Ahrberg, C. D., Choi, J. W., & Chung, B. G. (2018). Droplet-based synthesis of homogeneous magnetic iron oxide nanoparticles. *Beilstein J Nanotechnol, 9*, 2413-2420. https://doi.org/10.3762/bjnano.9.226

Ajinkya, N., Yu, X., Kaithal, P., Luo, H., Somani, P., & Ramakrishna, S. (2020). Magnetic Iron Oxide Nanoparticle (IONP) Synthesis to Applications: Present and Future. *Materials, 13*(20), 4644. https://www.mdpi.com/1996-1944/13/20/4644

Aktanova, A., Abramova, T., Pashkina, E., Boeva, O., Grishina, L., Kovalenko, E., & Kozlov, V. (2021). Assessment of the Biocompatibility of Cucurbiturils in Blood Cells. *Nanomaterials, 11*(6), 1356. https://www.mdpi.com/2079-4991/11/6/1356

Albert, F., Riccardo, Liberato, M., & Teresa, P. (2010). From iron oxide nanoparticles towards advanced iron-based inorganic materials designed for biomedical applications. *Pharmacological Research, 62*(2), 126-143. https://doi.org/https://doi.org/10.1016/j.phrs.2009.12.012

AlMatar, M., Makky, A. E., Var, I., & Koksal, F. (2018). The Role of Nanoparticles in the Inhibition of Multidrug-Resistant Bacteria and Biofilms. *Current Drug Delivery, 15*(4), 470-484. https://doi.org/http://dx.doi.org/10.2174/1567201815666171207163504

Anbu, P. (2022). Chemical synthesis of NiFe2O4/NG/cellulose nanocomposite and its antibacterial potential against bacterial pathogens. *Biotechnology and Applied Biochemistry, 69*(3), 867-875. https://doi.org/https://doi.org/10.1002/bab.2157

Ansari, S. A., Khan, M. M., Ansari, M. O., Lee, J., & Cho, M. H. (2013, 2013/12/27). Biogenic Synthesis, Photocatalytic, and Photoelectrochemical Performance of Ag–ZnO Nanocomposite. *The Journal of Physical Chemistry C, 117*(51), 27023-27030. https://doi.org/10.1021/jp410063p

Antibiotic resistance threats in the United States, 2019. (2019). [Report]. https://stacks.cdc.gov/view/cdc/82532

Arakha, M., Pal, S., Samantarrai, D., Panigrahi, T. K., Mallick, B. C., Pramanik, K., Mallick, B., & Jha, S. (2015, Oct 6). Antimicrobial activity of iron oxide nanoparticle upon modulation of nanoparticle-bacteria interface. *Sci Rep, 5*, 14813. https://doi.org/10.1038/srep14813

Arias, L. S., Pessan, J. P., Vieira, A. P. M., Lima, T. M. T., Delbem, A. C. B., & Monteiro, D. R. (2018, Jun 9). Iron Oxide Nanoparticles for Biomedical Applications: A Perspective on Synthesis, Drugs, Antimicrobial Activity, and Toxicity. *Antibiotics (Basel), 7*(2). https://doi.org/10.3390/antibiotics7020046

Armijo, L. M., Wawrzyniec, S. J., Kopciuch, M., Brandt, Y. I., Rivera, A. C., Withers, N. J., Cook, N. C., Huber, D. L., Monson, T. C., Smyth, H. D. C., & Osiński, M. (2020, Feb 18). Antibacterial activity of iron oxide, iron nitride, and tobramycin conjugated nanoparticles against Pseudomonas aeruginosa biofilms. *J Nanobiotechnology, 18*(1), 35. https://doi.org/10.1186/s12951-020-0588-6

Aruguete, D. M., & Hochella, M. F. (2010). Bacterianoparticle interactions and their environmental implications. *Environmental Chemistry, 7*(1), 3-9. https://doi.org/https://doi.org/10.1071/EN09115

Arulmurugan, R., Jeyadevan, B., Vaidyanathan, G., & Sendhilnathan, S. (2005, 2005/03/01/). Effect of zinc substitution on Co–Zn and Mn–Zn ferrite nanoparticles prepared by co-precipitation. *Journal of Magnetism and Magnetic Materials, 288*, 470-477. https://doi.org/https://doi.org/10.1016/j.jmmm.2004.09.138

Aslam, B., Wang, W., Arshad, M. I., Khurshid, M., Muzammil, S., Rasool, M. H., Nisar, M. A., Alvi, R. F., Aslam, M. A., Qamar, M. U., Salamat, M. K. F., & Baloch, Z. (2018). Antibiotic resistance: a rundown of a global crisis. *Infect Drug Resist, 11*, 1645-1658. https://doi.org/10.2147/idr.S173867

Azam, A., Ahmed, A. S., Oves, M., Khan, M. S., Habib, S. S., & Memic, A. (2012). Antimicrobial activity of metal oxide nanoparticles against Gram-positive and Gram-negative bacteria: a comparative study. *International journal of nanomedicine*, 6003-6009.

Babes, L., Denizot, B. t., Tanguy, G., Le Jeune, J. J., & Jallet, P. (1999, 1999/04/15/). Synthesis of Iron Oxide Nanoparticles Used as MRI Contrast Agents: A Parametric Study. *Journal of Colloid and Interface Science, 212*(2), 474-482. https://doi.org/https://doi.org/10.1006/jcis.1998.6053

Babu, A. T., Sebastian, M., Manaf, O., & Antony, R. (2020, 2020/06/01). Heterostructured Nanocomposites of Ag Doped Fe3O4 Embedded in ZnO for Antibacterial Applications and Catalytic Conversion of Hazardous Wastes. *Journal of Inorganic and Organometallic Polymers and Materials, 30*(6), 1944-1955. https://doi.org/10.1007/s10904-019-01366-y

Baek, Y. W., & An, Y. J. (2011, Mar 15). Microbial toxicity of metal oxide nanoparticles (CuO, NiO, ZnO, and Sb2O3) to Escherichia coli, Bacillus subtilis, and Streptococcus aureus. *Sci Total Environ, 409*(8), 1603-1608. https://doi.org/10.1016/j.scitotenv.2011.01.014

Bandi, S., Hastak, V., Pavithra, C., Kashyap, S., Singh, D., Luqman, S., Peshwe, D., & Srivastav, A. (2019, 09/20). Graphene/chitosan-functionalized iron oxide nanoparticles for biomedical applications. *Journal of Materials Research*. https://doi.org/10.1557/jmr.2019.267

Bauer, A. W., Kirby, W. M., Sherris, J. C., & Turck, M. (1966, Apr). Antibiotic susceptibility testing by a standardized single disk method. *Am J Clin Pathol, 45*(4), 493-496.

Bhattacharya, P., & Neogi, S. (2018, 08/30). Antibacterial properties of doped nanoparticles. *Reviews in Chemical Engineering, 35*. https://doi.org/10.1515/revce-2017-0116

Bhushan, M., Kumar, Y., Periyasamy, L., & Viswanath, A. K. (2019, 2019/03/01/). Study of synthesis, structural, optical and magnetic characterizations of iron/copper oxide nanocomposites: A promising novel inorganic antibiotic. *Materials Science and Engineering: C, 96*, 66-76. https://doi.org/https://doi.org/10.1016/j.msec.2018.11.009

Blair, J. M., Webber, M. A., Baylay, A. J., Ogbolu, D. O., & Piddock, L. J. (2015). Molecular mechanisms of antibiotic resistance. *Nature reviews microbiology, 13*(1), 42-51.

Borovanský, J., & Riley, P. A. (1989). Cytotoxicity of zinc in vitro. *Chem Biol Interact, 69*(2-3), 279-291. https://doi.org/10.1016/0009-2797(89)90085-9

Božić, L., Malinović, M., Gajić, D., Vračević, S., Pržulj, S., Jelić, D., & Šmitran, A. (2020). Study of Iron Oxide Nanoparticles Doped with Copper: Antimicrobal and Photocatalytical Activity. *Contemporary Materials, 11*(2). https://doi.org/10.7251/comen2002093j

Bulut, V. N., Duran, C., Gundogdu, A., Soylak, M., Yildirim, N., & Elci, L. (2008, 2008/07/15/). A new approach to separation and pre-concentration of some trace metals with co-precipitation method using a triazole. *Talanta, 76*(2), 469-474. https://doi.org/https://doi.org/10.1016/j.talanta.2008.03.040

Casula, M. F., Conca, E., Bakaimi, I., Sathya, A., Materia, M. E., Casu, A., Falqui, A., Sogne, E., Pellegrino, T., & Kanaras, A. G. (2016, Jun 22). Manganese doped-iron oxide nanoparticle clusters and their potential as agents for magnetic resonance imaging and hyperthermia. *Phys Chem Chem Phys, 18*(25), 16848-16855. https://doi.org/10.1039/c6cp02094a

Chand, P., Vaish, S., & Kumar, P. (2017, 2017/11/01/). Structural, optical and dielectric properties of transition metal (MFe2O4; M = Co, Ni and Zn) nanoferrites. *Physica B: Condensed Matter, 524*, 53-63. https://doi.org/https://doi.org/10.1016/j.physb.2017.08.060

Chia, C. H., Zakaria, S., Yusoff, M., Goh, S. C., Haw, C. Y., Ahmadi, S., Huang, N. M., & Lim, H. N. (2010, 2010/03/01/). Size and crystallinity-dependent magnetic properties of CoFe2O4 nanocrystals. *Ceramics International, 36*(2), 605-609. https://doi.org/https://doi.org/10.1016/j.ceramint.2009.10.001

Choi, O., Deng, K. K., Kim, N.-J., Ross, L., Surampalli, R. Y., & Hu, Z. (2008, 2008/06/01/). The inhibitory effects of silver nanoparticles, silver ions, and silver chloride colloids on microbial growth. *Water Research, 42*(12), 3066-3074. https://doi.org/https://doi.org/10.1016/j.watres.2008.02.021

Collignon, P., & Beggs, J. J. (2019). Socioeconomic Enablers for Contagion: Factors Impelling the Antimicrobial Resistance Epidemic. *Antibiotics, 8*(3), 86. https://www.mdpi.com/2079-6382/8/3/86

Correcher, R., Budyk, Y., & Fullana, A. (2021, Nov 9). Role of Gallic Acid in the Synthesis of Carbon-Encapsulated Iron Nanoparticles by Hydrothermal Carbonization: Selecting Iron Oxide Composition. *ACS Omega, 6*(44), 29547-29554. https://doi.org/10.1021/acsomega.1c03692

Cui, H., Zhu, G., Qiu, L., & Ye, X. (2021, 2021/09/01/). RETRACTED: Facile synthesis of Mg-doped calcium silicate porous nanoparticles for targeted drug delivery and ovarian cancer treatment. *Ceramics International, 47*(17), 24942-24948. https://doi.org/https://doi.org/10.1016/j.ceramint.2021.05.221

Darezereshki, E. (2011, 2011/02/28/). One-step synthesis of hematite (α-Fe2O3) nano-particles by direct thermal-decomposition of maghemite. *Materials Letters, 65*(4), 642-645. https://doi.org/https://doi.org/10.1016/j.matlet.2010.11.030

Das, S., Diyali, S., Vinothini, G., Perumalsamy, B., Balakrishnan, G., Ramasamy, T., Dharumadurai, D., & Biswas, B. (2020, 2020/09/01/). Synthesis, morphological analysis, antibacterial activity of iron oxide nanoparticles and the cytotoxic effect on lung cancer cell line. *Heliyon, 6*(9), e04953. https://doi.org/https://doi.org/10.1016/j.heliyon.2020.e04953

de Lacerda Coriolano, D., de Souza, J. B., Bueno, E. V., Medeiros, S., Cavalcanti, I. D. L., & Cavalcanti, I. M. F. (2021, Mar). Antibacterial and antibiofilm potential of silver nanoparticles against antibiotic-sensitive and multidrug-resistant Pseudomonas aeruginosa strains. *Braz J Microbiol, 52*(1), 267-278. https://doi.org/10.1007/s42770-020-00406-x

Dibrov, P., Dzioba, J., Gosink, K. K., & Häse, C. C. (2002). Chemiosmotic Mechanism of Antimicrobial Activity of Ag⁺ in Vibrio cholerae. *Antimicrobial Agents and Chemotherapy, 46*(8), 2668-2670. https://doi.org/doi:10.1128/aac.46.8.2668-2670.2002

Dobrovolskaia, M. A., Clogston, J. D., Neun, B. W., Hall, J. B., Patri, A. K., & McNeil, S. E. (2008, Aug). Method for analysis of nanoparticle hemolytic properties in vitro. *Nano Lett, 8*(8), 2180-2187. https://doi.org/10.1021/nl0805615

Doumandji, Z., Safar, R., Lovera-Leroux, M., Nahle, S., Cassidy, H., Matallanas, D., Rihn, B., Ferrari, L., & Joubert, O. (2020, Feb). Protein and lipid homeostasis altered in rat macrophages after exposure to metallic oxide nanoparticles. *Cell Biol Toxicol, 36*(1), 65-82. https://doi.org/10.1007/s10565-019-09484-6

Dutta, R. K., Nenavathu, B. P., Gangishetty, M. K., & Reddy, A. V. (2013). Antibacterial effect of chronic exposure of low concentration ZnO nanoparticles on E. coli. *J Environ Sci Health A Tox Hazard Subst Environ Eng, 48*(8), 871-878. https://doi.org/10.1080/10934529.2013.761489

Elayakumar, K., Dinesh, A., Manikandan, A., Palanivelu, M., Kavitha, G., Prakash, S., Thilak Kumar, R., Jaganathan, S. K., & Baykal, A. (2019, 2019/04/15/). Structural, morphological, enhanced magnetic properties and antibacterial bio-medical activity of rare earth element (REE) cerium (Ce3+) doped CoFe2O4 nanoparticles. *Journal of Magnetism and Magnetic Materials, 476*, 157-165. https://doi.org/https://doi.org/10.1016/j.jmmm.2018.09.089

Fang, M., Chen, J.-H., Xu, X.-L., Yang, P.-H., & Hildebrand, H. F. (2006, 2006/06/01/). Antibacterial activities of inorganic agents on six bacteria associated with oral infections by two susceptibility tests. *International Journal of Antimicrobial Agents, 27*(6), 513-517. https://doi.org/https://doi.org/10.1016/j.ijantimicag.2006.01.008

Farias, I. A. P., Dos Santos, C. C. L., & Sampaio, F. C. (2018). Antimicrobial Activity of Cerium Oxide Nanoparticles on Opportunistic Microorganisms: A Systematic Review. *Biomed Res Int, 2018*, 1923606. https://doi.org/10.1155/2018/1923606

Feng, X., Guo, H., Patel, K., Zhou, H., & Lou, X. (2014). High performance, recoverable Fe3O4ZnO nanoparticles for enhanced photocatalytic degradation of phenol. *Chemical Engineering Journal, 244*, 327-334.

Gabrielyan, L., Hovhannisyan, A., Gevorgyan, V., Ananyan, M., & Trchounian, A. (2019, 2019/03/01). Antibacterial effects of iron oxide (Fe3O4) nanoparticles: distinguishing concentration-dependent effects with different bacterial cells growth and membrane-associated mechanisms. *Applied Microbiology and Biotechnology, 103*(6), 2773-2782. https://doi.org/10.1007/s00253-019-09653-x

Gawande, M. B., Goswami, A., Felpin, F.-X., Asefa, T., Huang, X., Silva, R., Zou, X., Zboril, R., & Varma, R. S. (2016, 2016/03/23). Cu and Cu-Based Nanoparticles: Synthesis and Applications in Catalysis. *Chemical Reviews, 116*(6), 3722-3811. https://doi.org/10.1021/acs.chemrev.5b00482

Gu, H., Xu, K., Xu, C., & Xu, B. (2006, Mar 7). Biofunctional magnetic nanoparticles for protein separation and pathogen detection. *Chem Commun (Camb)*(9), 941-949. https://doi.org/10.1039/b514130c

Haase, H., Overbeck, S., & Rink, L. (2008, 2008/05/01/). Zinc supplementation for the treatment or prevention of disease: Current status and future perspectives. *Experimental Gerontology, 43*(5), 394-408. https://doi.org/https://doi.org/10.1016/j.exger.2007.12.002

Haghniaz, R., Rabbani, A., Vajhadin, F., Khan, T., Kousar, R., Khan, A. R., Montazerian, H., Iqbal, J., Libanori, A., Kim, H.-J., & Wahid, F. (2021, 2021/02/05). Anti-bacterial and wound healing-promoting effects of zinc ferrite nanoparticles. *Journal of Nanobiotechnology, 19*(1), 38. https://doi.org/10.1186/s12951-021-00776-w

Hajipour, M. J., Fromm, K. M., Ashkarran, A. A., Jimenez de Aberasturi, D., de Larramendi, I. R., Rojo, T., Serpooshan, V., Parak, W. J., & Mahmoudi, M. (2012, Oct). Antibacterial properties of nanoparticles. *Trends Biotechnol, 30*(10), 499-511. https://doi.org/10.1016/j.tibtech.2012.06.004

Hamidian, K., Sarani, M., Sheikhi, E., & Khatami, M. (2022). Cytotoxicity evaluation of green synthesized ZnO and Ag-doped ZnO nanoparticles on brain glioblastoma cells. *Journal of Molecular Structure, 1251*, 131962.

Hanusch, U., Mahmoudi, M., Maurizi, L., Salaklang, J., & Hofmann, H. (2014, 05/21). Protein Corona Composition of Superparamagnetic Iron Oxide Nanoparticles with Various Physico-Chemical Properties and Coatings. *Scientific Reports, 4*, 5020. https://doi.org/10.1038/srep05020

Hastak, V., Bandi, S., Kashyap, S., Singh, S., Luqman, S., Lodhe, M., Peshwe, D. R., & Srivastav, A. K. (2018, Sep 29). Antioxidant efficacy of chitosan/graphene functionalized superparamagnetic iron oxide nanoparticles. *J Mater Sci Mater Med, 29*(10), 154. https://doi.org/10.1007/s10856-018-6163-0

Hoque, S. M., Mehrin, T., Liba, S. I., Salehin, F., Mahmood, Z. H., Khan, M. N. I., Chattopadhayay, K., Rafiqul, I., & Akhter, S. (2016). Thermo-therapeutic applications of chitosan- and PEG-coated NiFe2O4 nanoparticles. *Nanotechnology, 27*(28), 285702. https://doi.org/10.1088/0957-4484/27/28/285702

Hoque, S. M., Srivastava, C., Venkatesha, N., Kumar, A., & Chattopadhyay, K. (2013, 05/01). Superparamagnetic behaviour and T 1, T 2 relaxivity of ZnFe2O4 nanoparticles for magnetic resonance imaging. *Philosophical Magazine, 93*. https://doi.org/10.1080/14786435.2012.755271

Houshiar, M., Zebhi, F., Razi, Z. J., Alidoust, A., & Askari, Z. (2014, 2014/12/01/). Synthesis of cobalt ferrite (CoFe2O4) nanoparticles using combustion, coprecipitation, and precipitation methods: A comparison study of size, structural, and magnetic properties. *Journal of Magnetism and Magnetic Materials, 371*, 43-48. https://doi.org/https://doi.org/10.1016/j.jmmm.2014.06.059

Humphries, R. M., Ambler, J., Mitchell, S. L., Castanheira, M., Dingle, T., Hindler, J. A., Koeth, L., & Sei, K. (2018, Apr). CLSI Methods Development and Standardization Working Group Best Practices for Evaluation of Antimicrobial Susceptibility Tests. *J Clin Microbiol, 56*(4). https://doi.org/10.1128/jcm.01934-17

Hussein-Al-Ali, S. H., El Zowalaty, M. E., Hussein, M. Z., Geilich, B. M., & Webster, T. J. (2014). Synthesis, characterization, and antimicrobial activity of an ampicillin-conjugated magnetic nanoantibiotic for medical applications. *Int J Nanomedicine, 9*, 3801-3814. https://doi.org/10.2147/ijn.S61143

Ika O. Wulandari, H. S., Anna Safitri, Dionysius J. D. H Santjojo , , Akhmad Sabarudin,. (2019). *Development of synthesis method of magnetic nanoparticles modified by oleic acid and chitosan as a candidate for drug delivery agent* (Vol. Volume: 9). Issue: 7. https://japsonline.com/bib_files/abstract.php?article_id=japs2936

Iriarte-Mesa, C., López, Y. C., Matos-Peralta, Y., de la Vega-Hernández, K., & Antuch, M. (2020, Jan 7). Gold, Silver and Iron Oxide Nanoparticles: Synthesis and Bionanoconjugation Strategies Aimed at Electrochemical Applications. *Top Curr Chem (Cham), 378*(1), 12. https://doi.org/10.1007/s41061-019-0275-y

Ismail, R. A., Sulaiman, G. M., Abdulrahman, S. A., & Marzoog, T. R. (2015, Aug). Antibacterial activity of magnetic iron oxide nanoparticles synthesized by laser ablation in liquid. *Mater Sci Eng C Mater Biol Appl, 53*, 286-297. https://doi.org/10.1016/j.msec.2015.04.047

Ivashchenko, O., Lewandowski, M., Peplińska, B., Jarek, M., Nowaczyk, G., Wiesner, M., Załęski, K., Babutina, T., Warowicka, A., & Jurga, S. (2015, Oct). Synthesis and characterization of magnetite/silver/antibiotic nanocomposites for targeted antimicrobial therapy. *Mater Sci Eng C Mater Biol Appl, 55*, 343-359. https://doi.org/10.1016/j.msec.2015.05.023

Ivashchenko, O., Woźniak, A., Coy, E., Peplinska, B., Gapinski, J., & Jurga, S. (2017, Apr 1). Release and cytotoxicity studies of magnetite/Ag/antibiotic nanoparticles: An interdependent relationship. *Colloids Surf B Biointerfaces, 152*, 85-94. https://doi.org/10.1016/j.colsurfb.2017.01.009

Jacinto, M. J., Silva, V. C., Valladão, D. M. S., & Souto, R. S. (2021, 2021/01/01). Biosynthesis of magnetic iron oxide nanoparticles: a review. *Biotechnology Letters, 43*(1), 1-12. https://doi.org/10.1007/s10529-020-03047-0

Jain, A. S., Pawar, P. S., Sarkar, A., Junnuthula, V., & Dyawanapelly, S. (2021, Nov 5). Bionanofactories for Green Synthesis of Silver Nanoparticles: Toward Antimicrobial Applications. *Int J Mol Sci, 22*(21). https://doi.org/10.3390/ijms222111993

Jaishankar, A., Jusufi, A., Vreeland, J. L., Deighton, S., Pellettiere, J., & Schilowitz, A. M. (2019, Feb 12). Adsorption of Stearic Acid at the Iron Oxide/Oil Interface: Theory, Experiments, and Modeling. *Langmuir, 35*(6), 2033-2046. https://doi.org/10.1021/acs.langmuir.8b03132

Janani, B., Al-Mohaimeed, A. M., Raju, L. L., Al Farraj, D. A., Thomas, A. M., & Khan, S. S. (2021, 2021/06/01). Synthesis and characterizations of hybrid PEG-Fe3O4 nanoparticles for the efficient adsorptive removal of dye and antibacterial, and antibiofilm applications. *Journal of Environmental Health Science and Engineering, 19*(1), 389-400. https://doi.org/10.1007/s40201-021-00612-1

Janczak, K., Kosmalska, D., Kaczor, D., Raszkowska-Kaczor, A., Wedderburn, L., & Malinowski, R. (2021). Bactericidal and Fungistatic Properties of LDPE Modified with a Biocide Containing Metal Nanoparticles. *Materials, 14*(15), 4228. https://www.mdpi.com/1996-1944/14/15/4228

Jiang, L., Wen, Y., Zhu, Z., Su, C., Ye, S., Wang, J., Liu, X., & Shao, W. (2020, 2020/02/15/). Construction of an efficient nonleaching graphene nanocomposites with enhanced contact antibacterial performance. *Chemical Engineering Journal, 382*, 122906. https://doi.org/https://doi.org/10.1016/j.cej.2019.122906

Jiang, Y., Zhang, L., Wen, D., & Ding, Y. (2016, Dec 1). Role of physical and chemical interactions in the antibacterial behavior of ZnO nanoparticles against E. coli. *Mater Sci Eng C Mater Biol Appl, 69*, 1361-1366. https://doi.org/10.1016/j.msec.2016.08.044

Jing, Z., & Wu, S. (2004, 11/01). Synthesis and characterization of monodisperse hematite nanoparticles modified by surfactants via hydrothermal approach. *Materials Letters, 58*, 3637-3640. https://doi.org/10.1016/j.matlet.2004.07.010

Jolivet, J.-P., Chanéac, C., & Tronc, E. (2004). Iron oxide chemistry. From molecular clusters to extended solid networks [10.1039/B304532N]. *Chemical Communications*(5), 481-483. https://doi.org/10.1039/B304532N

Kandasamy, G., Sudame, A., Bhati, P., Chakrabarty, A., Kale, S. N., & Maity, D. (2018, Mar 15). Systematic magnetic fluid hyperthermia studies of carboxyl functionalized hydrophilic superparamagnetic iron oxide nanoparticles based ferrofluids. *J Colloid Interface Sci, 514*, 534-543. https://doi.org/10.1016/j.jcis.2017.12.064

Karunakaran, C., Gomathisankar, P., & Manikandan, G. (2010, 2010/10/01/). Preparation and characterization of antimicrobial Ce-doped ZnO nanoparticles for photocatalytic detoxification of cyanide. *Materials Chemistry and Physics, 123*(2), 585-594. https://doi.org/https://doi.org/10.1016/j.matchemphys.2010.05.019

Keerthana, S. P., Yuvakkumar, R., Ravi, G., Kumar, P., Elshikh, M. S., Alkhamis, H. H., Alrefaei, A. F., & Velauthapillai, D. (2021, May). A strategy to enhance the photocatalytic efficiency of α-Fe(2)O(3). *Chemosphere, 270*, 129498. https://doi.org/10.1016/j.chemosphere.2020.129498

Khan, M. M., Harunsani, M. H., Tan, A. L., Hojamberdiev, M., Poi, Y. A., & Ahmad, N. (2020, 2020/12/01). Antibacterial Studies of ZnO and Cu-Doped ZnO Nanoparticles Synthesized Using Aqueous Leaf Extract of Stachytarpheta jamaicensis. *BioNanoScience, 10*(4), 1037-1048. https://doi.org/10.1007/s12668-020-00775-5

Khashan, K. S., Sulaiman, G. M., Hussain, S. A., Marzoog, T. R., & Jabir, M. S. (2020, 2020/09/01). Synthesis, Characterization and Evaluation of Anti-bacterial, Anti-parasitic and Anti-cancer Activities of Aluminum-Doped Zinc Oxide Nanoparticles. *Journal of Inorganic and Organometallic Polymers and Materials, 30*(9), 3677-3693. https://doi.org/10.1007/s10904-020-01522-9

Kohanski, M. A., DePristo, M. A., & Collins, J. J. (2010, Feb 12). Sublethal antibiotic treatment leads to multidrug resistance via radical-induced mutagenesis. *Mol Cell, 37*(3), 311-320. https://doi.org/10.1016/j.molcel.2010.01.003

Laha, S. S., Thorat, N. D., Singh, G., Sathish, C. I., Yi, J., Dixit, A., & Vinu, A. (2022, Mar). Rare-Earth Doped Iron Oxide Nanostructures for Cancer Theranostics: Magnetic Hyperthermia and Magnetic Resonance Imaging. *Small, 18*(11), e2104855. https://doi.org/10.1002/smll.202104855

Lallo da Silva, B., Abuçafy, M. P., Berbel Manaia, E., Oshiro Junior, J. A., Chiari-Andréo, B. G., Pietro, R. C. R., & Chiavacci, L. A. (2019). Relationship Between Structure And Antimicrobial Activity Of Zinc Oxide Nanoparticles: An Overview. *Int J Nanomedicine, 14*, 9395-9410. https://doi.org/10.2147/ijn.S216204

Laurent, S., Forge, D., Port, M., Roch, A., Robic, C., Vander Elst, L., & Muller, R. N. (2008, Jun). Magnetic iron oxide nanoparticles: synthesis, stabilization, vectorization, physicochemical characterizations, and biological applications. *Chem Rev, 108*(6), 2064-2110. https://doi.org/10.1021/cr068445e

Leung, Y. H., Chan, C. M. N., Ng, A. M. C., Chan, H. T., Chiang, M. W. L., Djurišić, A. B., Ng, Y. H., Jim, W. Y., Guo, M. Y., Leung, F. C. C., Chan, W. K., & Au, D. T. W. (2012, 2012/10/26). Antibacterial activity of ZnO nanoparticles with a modified surface under ambient illumination. *Nanotechnology, 23*(47), 475703. https://doi.org/10.1088/0957-4484/23/47/475703

Li, D., Shen, M., Xia, J., & Shi, X. (2021, Apr). Recent developments of cancer nanomedicines based on ultrasmall iron oxide nanoparticles and nanoclusters. *Nanomedicine (Lond), 16*(8), 609-612. https://doi.org/10.2217/nnm-2021-0033

Li, D., Shen, M., Xia, J., & Shi, X. (2021). Recent developments of cancer nanomedicines based on ultrasmall iron oxide nanoparticles and nanoclusters. *Nanomedicine, 16*(8), 609-612. https://doi.org/10.2217/nnm-2021-0033

Li, Q., Kartikowati, C. W., Horie, S., Ogi, T., Iwaki, T., & Okuyama, K. (2017, 2017/08/30). Correlation between particle size/domain structure and magnetic properties of highly crystalline Fe3O4 nanoparticles. *Scientific Reports, 7*(1), 9894. https://doi.org/10.1038/s41598-017-09897-5

Li, W., Wei, W., Wu, X., Zhao, Y., & Dai, H. (2020). The antibacterial and antibiofilm activities of mesoporous hollow Fe3O4 nanoparticles in an alternating magnetic field [10.1039/D0BM00673D]. *Biomaterials Science, 8*(16), 4492-4507. https://doi.org/10.1039/D0BM00673D

Li, Y., Bao, J., Bian, Y., Erben, U., Wang, P., Song, K., Liu, S., Li, Z., Gao, Z., & Qin, Z. (2018). S100A4(+) Macrophages Are Necessary for Pulmonary Fibrosis by Activating Lung Fibroblasts. *Front Immunol, 9*, 1776. https://doi.org/10.3389/fimmu.2018.01776

Li, Y., Yang, D., Wang, S., Li, C., Xue, B., Yang, L., Shen, Z., Jin, M., Wang, J., & Qiu, Z. (2018). The Detailed Bactericidal Process of Ferric Oxide Nanoparticles on E. coli. *Molecules, 23*(3), 606. https://www.mdpi.com/1420-3049/23/3/606

Li, Z., Tan, B., Allix, M., Cooper, A. I., & Rosseinsky, M. J. (2008, Feb). Direct coprecipitation route to monodisperse dual-functionalized magnetic iron oxide nanocrystals without size selection. *Small, 4*(2), 231-239. https://doi.org/10.1002/smll.200700575

Liang, S., Wang, Y., Yu, J., Zhang, C., Xia, J., & Yin, D. (2007, Dec). Surface modified superparamagnetic iron oxide nanoparticles: as a new carrier for bio-magnetically targeted therapy. *J Mater Sci Mater Med, 18*(12), 2297-2302. https://doi.org/10.1007/s10856-007-3130-6

Lin, R., Li, Y., MacDonald, T., Wu, H., Provenzale, J., Peng, X., Huang, J., Wang, L., Wang, A. Y., Yang, J., & Mao, H. (2017, Feb 1). Improving sensitivity and specificity of capturing and detecting targeted cancer cells with anti-biofouling polymer coated magnetic iron oxide nanoparticles. *Colloids Surf B Biointerfaces, 150*, 261-270. https://doi.org/10.1016/j.colsurfb.2016.10.026

Liu, H., Li, P., Lu, B., Wei, Y., & Sun, Y. (2009, 2009/07/01/). Transformation of ferrihydrite in the presence or absence of trace Fe(II): The effect of preparation procedures of ferrihydrite. *Journal of Solid State Chemistry, 182*(7), 1767-1771. https://doi.org/https://doi.org/10.1016/j.jssc.2009.03.030

Liu, J., Liu, K., Zhang, L., Zhong, M., Hong, T., Zhang, R., Gao, Y., Li, R., Xu, T., & Xu, Z. P. (2021, 2021/07/10/). Heat/pH-boosted release of 5-fluorouracil and albumin-bound paclitaxel from Cu-doped layered double hydroxide nanomedicine for synergistical chemo-photo-therapy of breast cancer. *Journal of Controlled Release, 335*, 49-58. https://doi.org/https://doi.org/10.1016/j.jconrel.2021.05.011

Liu, X., Liu, J., Zhang, S., Nan, Z., & Shi, Q. (2016, 2016/01/21). Structural, Magnetic, and Thermodynamic Evolutions of Zn-Doped Fe3O4 Nanoparticles Synthesized Using a One-Step Solvothermal Method. *The Journal of Physical Chemistry C, 120*(2), 1328-1341. https://doi.org/10.1021/acs.jpcc.5b10618

Liu, X., Ma, Z., Xing, J., & Liu, H. (2004, 2004/03/01/). Preparation and characterization of amino–silane modified superparamagnetic silica nanospheres. *Journal of Magnetism and Magnetic Materials, 270*(1), 1-6. https://doi.org/https://doi.org/10.1016/j.jmmm.2003.07.006

M. T. Bell, A., Nicholas B. Smith, J., Paul Attfield, J., M. Rawson, J., Shankland, K., & I. F. David, W. (1999). A synchrotron X-ray powder diffraction study of 4-(2,3,4-trifluorophenyl)-1,2,3,5-dithiadiazolyl. Crystal structure determination using a global optimisation method [10.1039/A902534K]. *New Journal of Chemistry, 23*(6), 565-567. https://doi.org/10.1039/A902534K

Manaargadoo-Catin, M., Ali-Cherif, A., Pougnas, J.-L., & Perrin, C. (2016, 2016/02/01/). Hemolysis by surfactants — A review. *Advances in Colloid and Interface Science, 228*, 1-16. https://doi.org/https://doi.org/10.1016/j.cis.2015.10.011

Martínez-Rodríguez, N. L., Tavárez, S., & González-Sánchez, Z. I. (2019, Jun). In vitro toxicity assessment of zinc and nickel ferrite nanoparticles in human erythrocytes and peripheral blood mononuclear cell. *Toxicol In Vitro, 57*, 54-61. https://doi.org/10.1016/j.tiv.2019.02.011

Mikhnavets, L., Abashkin, V., Khamitsevich, H., Shcharbin, D., Burko, A., Krekoten, N., & Radziuk, D. (2022, Mar 14). Ultrasonic Formation of Fe(3)O(4)-Reduced Graphene Oxide-Salicylic Acid Nanoparticles with Switchable Antioxidant Function. *ACS Biomater Sci Eng, 8*(3), 1181-1192. https://doi.org/10.1021/acsbiomaterials.1c01603

Mohamed, H. E. A., Afridi, S., Khalil, A. T., Ali, M., Zohra, T., Salman, M., Ikram, A., Shinwari, Z. K., & Maaza, M. (2020, 2020/07/01/). Bio-redox potential of Hyphaene thebaica in bio-fabrication of ultrafine maghemite phase iron oxide nanoparticles (Fe2O3 NPs) for therapeutic applications. *Materials Science and Engineering: C, 112*, 110890. https://doi.org/https://doi.org/10.1016/j.msec.2020.110890

Mohammadi, M. R., Malkovskiy, A., Jothimuthu, P., Kim, K.-M., Parekh, M., Inayathullah, M., Zhuge, Y., & Rajadas, J. (2018, 03/09). PEG/Dextran Double Layer Influences Fe Ion Release and Colloidal Stability of Iron Oxide Nanoparticles. *Scientific Reports, 8*. https://doi.org/10.1038/s41598-018-22644-8

Mohtar, S. S., Aziz, F., Ismail, A. F., Sambudi, N. S., Abdullah, H., Rosli, A. N., & Ohtani, B. (2021). Impact of Doping and Additive Applications on Photocatalyst Textural Properties

in Removing Organic Pollutants: A Review. *Catalysts, 11*(10), 1160. https://www.mdpi.com/2073-4344/11/10/1160

Mondal, R., Polash, S. A., Saha, T., Islam, Z., Sikder, M. M., Alam, N., Hossain, M. S., & Sarker, S. R. (2017). Investigation of the Phytoconstituents and Bioactivity of Various Parts of Wild Type and Cultivated <i>Phyllanthus emblica</i> L. *Advances in Bioscience and Biotechnology, Vol.08No.07*, 17, Article 77426. https://doi.org/10.4236/abb.2017.87016

Mussin, J., Robles-Botero, V., Casañas-Pimentel, R., Rojas, F., Angiolella, L., San Martín-Martínez, E., & Giusiano, G. (2021, Jul 15). Antimicrobial and cytotoxic activity of green synthesis silver nanoparticles targeting skin and soft tissue infectious agents. *Sci Rep, 11*(1), 14566. https://doi.org/10.1038/s41598-021-94012-y

Nallathamby, P. D., Lee, K. J., Desai, T., & Xu, X.-H. N. (2010, 2010/07/20). Study of the Multidrug Membrane Transporter of Single Living Pseudomonas aeruginosa Cells Using Size-Dependent Plasmonic Nanoparticle Optical Probes. *Biochemistry, 49*(28), 5942-5953. https://doi.org/10.1021/bi100268k

Neely, A. N., & Holder, I. A. (1999). Antimicrobial resistance. *Burns: Journal of the International Society for Burn Injuries, 25*(1), 17-24.

Nigam, S., Barick, K., & Bahadur, D. (2011, 01/31). Development of citrate-stabilized Fe3O4 nanoparticles: Conjugation and release of doxorubicin for therapeutic applications. *Journal of Magnetism and Magnetic Materials - J MAGN MAGN MATER, 323*, 237-243. https://doi.org/10.1016/j.jmmm.2010.09.009

Noqta, O. A., Aziz, A. A., Usman, I. A., & Bououdina, M. (2019, 2019/04/01). Recent Advances in Iron Oxide Nanoparticles (IONPs): Synthesis and Surface Modification for Biomedical Applications. *Journal of Superconductivity and Novel Magnetism, 32*(4), 779-795. https://doi.org/10.1007/s10948-018-4939-6

Nosrati, H., Salehiabar, M., Davaran, S., Ramazani, A., Manjili, H. K., & Danafar, H. (2017). New advances strategies for surface functionalization of iron oxide magnetic nano particles (IONPs). *Research on Chemical Intermediates, 43*, 7423-7442.

O'Neill, J. (2016). *Tackling drug-resistant infections globally: final report and recommendations* [Report]. Government of the United Kingdom. https://apo.org.au/node/63983

Omelchenko, A. I., Sobol, E. N., Simakin, A. V., Serkov, A. A., Sukhov, I. A., & Shafeev, G. A. (2015). Biofunctional magnetic 'core–shell' nanoparticles generated by laser ablation of iron in liquid. *Laser Physics, 25*(2), 025607. https://doi.org/10.1088/1054-660X/25/2/025607

Organization, W. H. (2021). Global antimicrobial resistance and use surveillance system (GLASS) report: 2021.

Padwal, P., Bandyopadhyaya, R., & Mehra, S. (2014, 2014/12/23). Polyacrylic Acid-Coated Iron Oxide Nanoparticles for Targeting Drug Resistance in Mycobacteria. *Langmuir, 30*(50), 15266-15276. https://doi.org/10.1021/la503808d

Plaper, A., Jenko-Brinovec, S., Premzl, A., Kos, J., & Raspor, P. (2002, Jul). Genotoxicity of trivalent chromium in bacterial cells. Possible effects on DNA topology. *Chem Res Toxicol, 15*(7), 943-949. https://doi.org/10.1021/tx010096q

Pokhrel, L. R., Jacobs, Z. L., Dikin, D., & Akula, S. M. (2022, Apr 25). Five nanometer size highly positive silver nanoparticles are bactericidal targeting cell wall and adherent fimbriae expression. *Sci Rep, 12*(1), 6729. https://doi.org/10.1038/s41598-022-10778-9

Prabhakaran, T., Mangalaraja, R. V., Denardin, J. C., & Jiménez, J. A. (2017, 2017/05/01/). The effect of reaction temperature on the structural and magnetic properties of nano CoFe2O4. *Ceramics International, 43*(7), 5599-5606. https://doi.org/https://doi.org/10.1016/j.ceramint.2017.01.092

Prabhu, Y. T., Rao, K. V., Kumari, B. S., Kumar, V. S. S., & Pavani, T. (2015, 2015/06/01). Synthesis of Fe3O4 nanoparticles and its antibacterial application. *International Nano Letters, 5*(2), 85-92. https://doi.org/10.1007/s40089-015-0141-z

Qi, J., Lan, H., Liu, R., Liu, H., & Qu, J. (2020, 2020/03/15/). Efficient Microcystis aeruginosa removal by moderate photocatalysis-enhanced coagulation with magnetic Zn-doped Fe3O4 particles. *Water Research, 171*, 115448. https://doi.org/https://doi.org/10.1016/j.watres.2019.115448

Rabia, I., Kamran, T., Baoshan, L., Aftab, A., Azka, & Sadia, N. (2017). Antibacterial activity of biochemically capped iron oxide nanoparticles: A view towards green chemistry. *Journal of Photochemistry and Photobiology B: Biology, 170*, 241-246. https://doi.org/https://doi.org/10.1016/j.jphotobiol.2017.04.020

Rahdar, A., Beyzaei, H., Saadat, M., Yu, X., & Trant, J. F. (2020). Synthesis, physical characterization, and antifungal and antibacterial activities of oleic acid capped nanomagnetite and cobalt-doped nanomagnetite. *Canadian Journal of Chemistry, 98*(1), 34-39. https://doi.org/10.1139/cjc-2019-0268

Rai, M. (2013). Nanobiotecnologia verde: biossínteses de nanopartículas metálicas e suas aplicações como nanoantimicrobianos. *Ciência e Cultura, 65*, 44-48. http://cienciaecultura.bvs.br/scielo.php?script=sci_arttext&pid=S0009-67252013000300014&nrm=iso

Raveesha, H. R., Bharath, H. L., Vasudha, D. R., Sushma, B. K., Pratibha, S., & Dhananjaya, N. (2021). Antibacterial and antiproliferation activity of green synthesized nanoparticles from rhizome extract of Alpinia galangal (L.) Wild. *Inorganic Chemistry Communications, 132*, 108854. https://doi.org/https://doi.org/10.1016/j.inoche.2021.108854

Rayman, M. P. (2000). The importance of selenium to human health. *The lancet, 356*(9225), 233-241.

Rekha, K., Nirmala, M., Nair, M. G., & Anukaliani, A. (2010, 2010/08/01/). Structural, optical, photocatalytic and antibacterial activity of zinc oxide and manganese doped zinc oxide nanoparticles. *Physica B: Condensed Matter, 405*(15), 3180-3185. https://doi.org/https://doi.org/10.1016/j.physb.2010.04.042

Rivas Rojas, P., Tancredi, P., Moscoso Londoño, O., Knobel, M., & Socolovsky, L. (2017, 11/01). Tuning dipolar magnetic interactions by controlling individual silica coating of iron oxide nanoparticles. *Journal of Magnetism and Magnetic Materials, 451*. https://doi.org/10.1016/j.jmmm.2017.11.099

Rufus, A., N, S., & Philip, D. (2016). Synthesis of biogenic hematite (α-Fe2O3) nanoparticles for antibacterial and nanofluid applications [10.1039/C6RA20240C]. *RSC Advances, 6*(96), 94206-94217. https://doi.org/10.1039/C6RA20240C

Sadeghi Rad, T., Khataee, A., Vafaei, F., & Rahim Pouran, S. (2021, 2021/07/01/). Chromium and cerium co-doped magnetite/reduced graphene oxide nanocomposite as a potent antibacterial agent against S. aureus. *Chemosphere, 274*, 129988. https://doi.org/https://doi.org/10.1016/j.chemosphere.2021.129988

Saikia, C., Das, M. K., Ramteke, A., & Maji, T. K. (2016, Dec). Effect of crosslinker on drug delivery properties of curcumin loaded starch coated iron oxide nanoparticles. *Int J Biol Macromol, 93*(Pt A), 1121-1132. https://doi.org/10.1016/j.ijbiomac.2016.09.043

Saliani, M., Jalal, R., & Kafshdare. Goharshadi, E. (2015a). Effects of pH and Temperature on Antibacterial Activity of Zinc Oxide Nanofluid Against Escherichia coli O157: H7 and Staphylococcus aureus [Research Article]. *8*(2), e17115. https://doi.org/10.5812/jjm.17115

Saliani, M., Jalal, R., & Kafshdare. Goharshadi, E. (2015b). Effects of pH and Temperature on Antibacterial Activity of Zinc Oxide Nanofluid Against Escherichia coli O157: H7 and Staphylococcus aureus [Research Article]. *Jundishapur J Microbiol, 8*(2), e17115. https://doi.org/10.5812/jjm.17115

Seil, J. T., & Webster, T. J. (2012). Antimicrobial applications of nanotechnology: methods and literature. *Int J Nanomedicine, 7*, 2767-2781. https://doi.org/10.2147/ijn.S24805

Seil, J. T., & Webster, T. J. (2012, 2012/12/01). Antimicrobial applications of nanotechnology: methods and literature. *International journal of nanomedicine, 7*, 2767-2781. https://doi.org/10.2147/IJN.S24805

Shah, S. T., W, A. Y., Saad, O., Simarani, K., Chowdhury, Z., A, A. A., & Al-Ani, L. A. (2017, Oct 5). Surface Functionalization of Iron Oxide Nanoparticles with Gallic Acid as Potential Antioxidant and Antimicrobial Agents. *Nanomaterials (Basel), 7*(10). https://doi.org/10.3390/nano7100306

Shakil, M. S., Hasan, M. A., Uddin, M. F., Islam, A., Nahar, A., Das, H., Khan, M. N. I., Dey, B. P., Rokeya, B., & Hoque, S. M. (2020, 2020/11/16). In Vivo Toxicity Studies of Chitosan-Coated Cobalt Ferrite Nanocomplex for Its Application as MRI Contrast Dye. *ACS Applied Bio Materials, 3*(11), 7952-7964. https://doi.org/10.1021/acsabm.0c01069

Sharma, R. P., Raut, S. D., Jadhav, V. V., Mulani, R. M., Kadam, A. S., & Mane, R. S. (2022, 2022/10/01). Assessment of antibacterial and anti-biofilm effects of zinc ferrite nanoparticles against Klebsiella pneumoniae. *Folia Microbiologica, 67*(5), 747-755. https://doi.org/10.1007/s12223-022-00969-2

Shi, L.-E., Li, Z.-H., Zheng, W., Zhao, Y.-F., Jin, Y.-F., & Tang, Z.-X. (2014). Synthesis, antibacterial activity, antibacterial mechanism and food applications of ZnO nanoparticles: a review. *Food Additives & Contaminants: Part A, 31*(2), 173-186.

Shoaib, M., Bahadur, A., Iqbal, S., Al-Anazy, M. M., Laref, A., Tahir, M. A., Channar, P. A., Noreen, S., Yasir, M., Iqbal, A., & Ali, K. W. (2021, 2021/06/15/). Magnesium doped mesoporous bioactive glass nanoparticles: A promising material for apatite formation and mitomycin c delivery to the MG-63 cancer cells. *Journal of Alloys and Compounds, 866*, 159013. https://doi.org/https://doi.org/10.1016/j.jallcom.2021.159013

Shujah, T., Shahzadi, A., Haider, A., Mustajab, M., Haider, A. M., Ul-Hamid, A., Haider, J., Nabgan, W., & Ikram, M. (2022). Molybdenum-doped iron oxide nanostructures synthesized via a chemical co-precipitation route for efficient dye degradation and antimicrobial performance: in silico molecular docking studies [10.1039/D2RA07238F]. *RSC Advances, 12*(54), 35177-35191. https://doi.org/10.1039/D2RA07238F

Sihem, L., Hanine, D., & Faiza, B. (2020, 2020/03/01). Antibacterial Activity of α-Fe2O3 and α-Fe2O3@Ag Nanoparticles Prepared by Urtica Leaf Extract. *Nanotechnologies in Russia, 15*(2), 198-203. https://doi.org/10.1134/S1995078020020135

Silvia, G., Raja, S., Thivaharan, V., & Ramesh, V. (2017). Structural characterization, antibacterial and catalytic effect of iron oxide nanoparticles synthesised using the leaf extract of Cynometra ramiflora. *Journal of Molecular Structure, 1128*, 572-578. https://doi.org/https://doi.org/10.1016/j.molstruc.2016.09.031

Stanić, V., Dimitrijević, S., Antić-Stanković, J., Mitrić, M., Jokić, B., Plećaš, I. B., & Raičević, S. (2010, 2010/08/01/). Synthesis, characterization and antimicrobial activity of copper and zinc-doped hydroxyapatite nanopowders. *Applied Surface Science, 256*(20), 6083-6089. https://doi.org/https://doi.org/10.1016/j.apsusc.2010.03.124

Stein, R., Friedrich, B., Mühlberger, M., Cebulla, N., Schreiber, E., Tietze, R., Cicha, I., Alexiou, C., Dutz, S., Boccaccini, A. R., & Unterweger, H. (2020, Sep 26). Synthesis and Characterization of Citrate-Stabilized Gold-Coated Superparamagnetic Iron Oxide Nanoparticles for Biomedical Applications. *Molecules, 25*(19). https://doi.org/10.3390/molecules25194425

Stepien, G., Moros, M., Pérez-Hernández, M., Monge, M., Gutiérrez, L., Fratila, R. M., Las Heras, M., Menao Guillén, S., Puente Lanzarote, J. J., Solans, C., Pardo, J., & de la Fuente, J. M. (2018, Feb 7). Effect of Surface Chemistry and Associated Protein Corona on the Long-Term Biodegradation of Iron Oxide Nanoparticles In Vivo. *ACS Appl Mater Interfaces, 10*(5), 4548-4560. https://doi.org/10.1021/acsami.7b18648

Sugarman, B. (1983). Zinc and Infection. *Reviews of Infectious Diseases, 5*(1), 137-147. https://doi.org/10.1093/clinids/5.1.137

Sultan, M. Z., Jamil, Y., Javed, Y., & Sarfraz, R. A. (2021, 2021/12/01). Synthesis, Characterization, and Study of Thermal Response of Cu-Doped Fe3O4 Nanoparticles. *Journal of Superconductivity and Novel Magnetism, 34*(12), 3209-3221. https://doi.org/10.1007/s10948-021-05990-z

Tacconelli, E., & Pezzani, M. D. (2019). Public health burden of antimicrobial resistance in Europe. *The Lancet Infectious Diseases, 19*(1), 4-6.

Taei, M., Salavati, H., Hasanpour, F., Habibollahi, S., & Baghlani, H. (2016, Dec 1). Simultaneous determination of ascorbic acid, acetaminophen and codeine based on multi-walled carbon nanotubes modified with magnetic nanoparticles paste electrode. *Mater Sci Eng C Mater Biol Appl, 69*, 1-11. https://doi.org/10.1016/j.msec.2016.06.014

Toropova, Y. G., Zelinskaya, I. A., Gorshkova, M. N., Motorina, D. S., Korolev, D. V., Velikonivtsev, F. S., & Gareev, K. G. (2021, Oct). Albumin covering maintains endothelial function upon magnetic iron oxide nanoparticles intravenous injection in rats. *J Biomed Mater Res A, 109*(10), 2017-2026. https://doi.org/10.1002/jbm.a.37193

Tran, N., Mir, A., Mallik, D., Sinha, A., Nayar, S., & Webster, T. J. (2010, Apr 15). Bactericidal effect of iron oxide nanoparticles on Staphylococcus aureus. *Int J Nanomedicine, 5*, 277-283. https://doi.org/10.2147/ijn.s9220

Trindade, T., & Thomas, P. J. (2013). 4.13 - Defining and Using Very Small Crystals. In J. Reedijk & K. Poeppelmeier (Eds.), *Comprehensive Inorganic Chemistry II (Second Edition)* (pp. 343-369). Elsevier. https://doi.org/https://doi.org/10.1016/B978-0-08-097774-4.00416-2

Tringides, M. C., Jałochowski, M., & Bauer, E. (2007). Quantum size effects in metallic nanostructures. *Physics Today, 60*(4), 50-54. https://doi.org/10.1063/1.2731973

Vazquez-Muñoz, R., Meza-Villezcas, A., Fournier, P. G. J., Soria-Castro, E., Juarez-Moreno, K., Gallego-Hernández, A. L., Bogdanchikova, N., Vazquez-Duhalt, R., & Huerta-Saquero, A. (2019). Enhancement of antibiotics antimicrobial activity due to the silver nanoparticles impact on the cell membrane. *PLOS ONE, 14*(11), e0224904. https://doi.org/10.1371/journal.pone.0224904

Vedernikova, I. A. (2015, 2015/07/01). Magnetic nanoparticles: Advantages of using, methods for preparation, characterization, application in pharmacy. *Review Journal of Chemistry, 5*(3), 256-280. https://doi.org/10.1134/S2079978015030036

Vijayalakshmi, K., & L. (2021). Microwave-sonochemical synergistically assisted synthesis of hybrid Ni-Fe3O4/ZnO nanocomposite for enhanced antibacterial performance. *Materials Today Communications, 26*, 101835. https://doi.org/https://doi.org/10.1016/j.mtcomm.2020.101835

Vinosha, P. A., Manikandan, A., Judith Ceicilia, A. S., Dinesh, A., Francisco Nirmala, G., Preetha, A. C., Slimani, Y., Almessiere, M. A., Baykal, A., & Xavier, B. (2021, 2021/04/15/). Review on recent advances of zinc substituted cobalt ferrite nanoparticles: Synthesis characterization and diverse applications. *Ceramics International, 47*(8), 10512-10535. https://doi.org/https://doi.org/10.1016/j.ceramint.2020.12.289

Wang, H., Qin, X. Y., Li, Z. Y., Zheng, Z. Z., & Fan, T. Y. (2018, Apr 18). [Preparation and characterization of citric acid-modified superparamagnetic iron oxide nanoparticles]. *Beijing Da Xue Xue Bao Yi Xue Ban, 50*(2), 340-346.

Wright, G. D. (2010). Q&A: Antibiotic resistance: where does it come from and what can we do about it? *BMC biology, 8*, 1-6.

Xia, T., Wang, J., Wu, C., Meng, F., Shi, Z., Lian, J., Feng, J., & Meng, J. (2012). Novel complex-coprecipitation route to form high quality triethanolamine-coated Fe3O4 nanocrystals: Their high saturation magnetizations and excellent water treatment properties [10.1039/C2CE25813G]. *CrystEngComm, 14*(18), 5741-5744. https://doi.org/10.1039/C2CE25813G

Yaqoob, A. A., Safian, M. T.-u., Rashid, M., Parveen, T., Umar, K., & Ibrahim, M. N. M. (2021). Chapter One - Introduction of smart polymer nanocomposites. In S. A. Bhawani, A. Khan, & M. Jawaid (Eds.), *Smart Polymer Nanocomposites* (pp. 1-25). Woodhead Publishing. https://doi.org/https://doi.org/10.1016/B978-0-12-819961-9.00007-4

Yu, B., Wang, Z., Almutairi, L., Huang, S., & Kim, M. H. (2020, Feb). Harnessing iron-oxide nanoparticles towards the improved bactericidal activity of macrophage against Staphylococcus aureus. *Nanomedicine, 24*, 102158. https://doi.org/10.1016/j.nano.2020.102158

Yu, J., Zhang, W., Li, Y., Wang, G., Yang, L., Jin, J., Chen, Q., & Huang, M. (2015, 2014/12/22). Synthesis, characterization, antimicrobial activity and mechanism of a novel hydroxyapatite whisker/nano zinc oxide biomaterial. *Biomedical Materials, 10*(1), 015001. https://doi.org/10.1088/1748-6041/10/1/015001

Yu, L., Yin, Y., Mayers, B., & Xia, Y. (2002, 03/01). Modifying the Surface Properties of Superparamagnetic Iron Oxide Nanoparticles through A Sol-Gel Approach. *Nano Letters, 2*, 183-186. https://doi.org/10.1021/nl015681q

Zahraei, M., Monshi, A., Morales, M. d. P., Shahbazi-Gahrouei, D., Amirnasr, M., & Behdadfar, B. (2015, 2015/11/01/). Hydrothermal synthesis of fine stabilized superparamagnetic nanoparticles of Zn2+ substituted manganese ferrite. *Journal of Magnetism and Magnetic Materials, 393*, 429-436. https://doi.org/https://doi.org/10.1016/j.jmmm.2015.06.006

Žalnėravičius, R., Mikalauskaitė, A., Niaura, G., Paškevičius, A., & Jagminas, A. (2019, 2019/09/01/). Ultra-small methionine-capped Au0/Au+ nanoparticles as efficient drug against the antibiotic-resistant bacteria. *Materials Science and Engineering: C, 102*, 646-652. https://doi.org/https://doi.org/10.1016/j.msec.2019.04.062

Zhang, W., Ohno, S., Steer, B., Klee, S., Staab-Weijnitz, C. A., Wagner, D., Lehmann, M., Stoeger, T., Königshoff, M., & Adler, H. (2018, 2018-June-01). S100a4 Is Secreted by Alternatively Activated Alveolar Macrophages and Promotes Activation of Lung Fibroblasts in Pulmonary Fibrosis [Original Research]. *Frontiers in Immunology, 9*. https://doi.org/10.3389/fimmu.2018.01216

Zhang, X., Song, H., Yu, L., Wang, T., Xinguang, R., Kong, X., Xie, Y., & Wang, X. (2006, 2006/06/01/). Surface states and its influence on luminescence in ZnS nanocrystallite. *Journal of Luminescence, 118*(2), 251-256. https://doi.org/https://doi.org/10.1016/j.jlumin.2005.07.003

Zhang, Z. Q., & Song, S. C. (2016, Nov). Thermosensitive/superparamagnetic iron oxide nanoparticle-loaded nanocapsule hydrogels for multiple cancer hyperthermia. *Biomaterials, 106*, 13-23. https://doi.org/10.1016/j.biomaterials.2016.08.015